Final thesis in veterinary medicine: Systemic toxoplasmosis in striped dolphins stranded in the Canary Islands

Author: María Falcón Santana

Tutor: Eva María Sierra Pulpillo

Collaborating tutor: Manuel Arbelo Hernández

Academic year: 2018-2023

Convocatory: Ordinary

UNIVERSIDAD DE LAS PALMAS DE GRAN CANARIA
Facultad de Veterinaria

TABLE OF CONTENTS

ABSTRACT

Toxoplasma gondii is considered a major cause of death and encephalitis in marine mammals (*Dubey et al., 2003*), as well as is a reflection of the increased level of aquatic pollution (*Dubey et al., 2020*).

We present, for the first time, *T. gondii* infection in striped dolphins (*Stenella coeruleoalba*) stranded in the Canary Islands. Between 2000 and 2020, 1183 cetaceans were found stranded in the Canary coasts, 217 of them belonging to the species *Stenella coeruleoalba*, of which 167 were subjected to a complete anatomopathological study, two of them being relevant in our study.

Both animals (two males; adult and subdadult, respectively) showed poor body condition and lesions consistent with multiorgan necrosis and lymphohistiocytic inflammation with intralesional protozoa; specifically in the central nervous system, heart, rete mirabile, adrenal glands, pancreas, liver, lung, spleen and pituitary gland. However, in the adult specimen, chronic lymphoplasmacytic interstitial bronchopneumonia and multinodal follicular depletion with reactive lymphoid hyperplasia of the laryngeal and pharyngeal tonsils were also found. Meanwhile, in the subadult specimen, necrosis in the adenohypophysis, multinodal follicular depletion, focal ulcerative glossitis, focal ulcerative gastritis, multiorgan parasitosis and fractures in the mandible and tympanic-periotic complex, possibly caused by previous trauma, were also found. Despite the presence of other findings, the main lesions were compatible with systemic toxoplasmosis, as the cause of death in these striped dolphins.

The identification of *T. gondii* was confirmed by molecular methods. However, morbillivirus nucleic acid was not detected in the tissues of any of the dolphins, supporting the hypothesis that this protozoan played a primary etiologic role in the development of severe lesions in cetaceans.

This study therefore describes in detail the histopathological findings associated with *T. gondii* parasitosis in two striped dolphins and report severe extensive coagulative necrosis in the pancreas and the pituitary gland, two lesions not previously reported in cetaceans toxoplasmosis.

1. INTRODUCTION

Marine mammals are exposed to changes in the aquatic environment, either by climate change or environmental degradation, or by human action through chemical pollution (due to waste dumping) or noise pollution (due to the civilian and/or military use of sonar, among others) (*Dierauf et al., 2018*). Therefore, cetaceans will be stressed by environmental factors, which can be anthropogenic, such as fishing, tourism, or maritime traffic, or non-anthropogenic, caused for example by pathogens or biotoxins *(Díaz-Delgado et al., 2018).*

The volcanic origin of the Canary Islands and their geographical position are the most important factor for the distribution and variety of marine species inhabiting the archipelago *(Moro Abad et al., 2003).* Likewise, thanks to its oceanographic characteristics (temperature, depth, etc.), the migratory routes and presence of many marine species are favoured *(Dierauf et al., 2018).* In this sense, the Canary Islands have the highest biodiversity of cetaceans of the European coast with 31 species, 7 belonging to mysticetes and 24 to odontocetes (*BIOTA, Banco de Datos de Biodiversidad de Canarias).*

Cetaceans stranded on the coast are an extremely valued source of information of the biology, anatomy, physiology, and pathology of these marine mammals. Therefore, it is relevant to know the data obtained by the studies carried out on cetaceans stranded in the Canary Islands, as they provide crucial information about the health of the populations necessary to stablish conservation policies.

Toxoplasmosis is a zoonotic disease affecting both terrestrial and marine species and is believed to be an opportunistic pathogen in marine mammals *(Migaki et al., 1990). T. gondii*, together with morbillivirus, herpesvirus, poxvirus, *Brucella spp*. and *Paracoccidioides*, are among the most identified parasites in cetaceans *(Díaz-Delgado et al., 2018).*

1.1. Bibliographic review

Systemic toxoplasmosis is a disease caused by *Toxoplasma gondii (Apicomplexa* family), an obligate intracellular protozoan parasite, that survives in the cells of their hosts (Kochanoowsky and Koshy, 2018).

1.1.1. *Toxoplasma gondii*

1.1.1.1. Life Cycle

Its life cycle presents both sexual and asexual phases. The sexual cycle (gametogonia) begins when the definitive host, only the felids, ingests any of the three forms of the parasite (sporozoites, tachyzoites or bradyzoites). In the feline intestinal epithelium, *T. gondii* will give rise to male and female gametocytes. In addition, oocysts without sporulation, containing four haploid sporozoites, are shed in the feces (Kochanoowsky and Koshy, 2018). One to five days after excretion, sporulation occurs with the formation of two sporocysts, each with four sporozoites, within the oocysts. The oocyst wall (Figure 1) is quite resistant, so they will remain infective for years (*Dubey et al., 1998*).

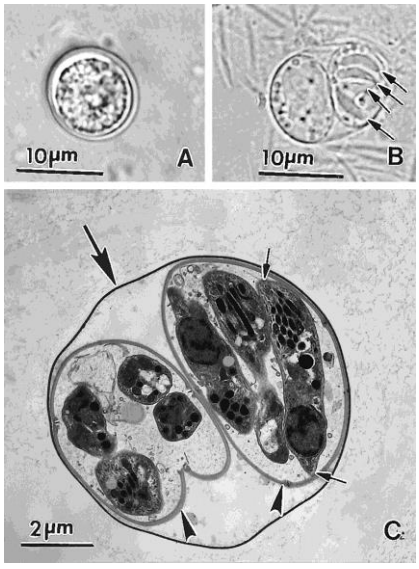

Figure 1. (A) Non-sporulated oocyst of *Toxoplasma gondii*. (B) Sporulated oocyst of *T. gondii* with two sporocysts and four sporozoites. (C) Sporulated oocyst of *T. gondii*. *Dubey, J. B., Lindsay, D. S., CA Speer, C. A. Structures of Toxoplasma gondii, Tachyzoites, Bradyzoites, and Sporozoites and Biology and Development of Tissue Cysts 1998.*

On the other side, *T. gondii* can also infect a wide variety of warm-blooded intermediate hosts, from birds to humans, through the ingestion of water, vegetables and/or fruits with presence of sporulated oocysts, ingestion of raw or undercooked meat with presence of cysts,

through the placenta in the case of humans, blood transfusion and/or transplantation of organs with presence of cysts or tachyzoites (*Attias et al., 2020)*. In such hosts, asexual reproduction of the parasite will take place (endodiogeny) giving rise to two daughter cells within the mother cell that will eventually separate (Kochanoowsky and Koshy, 2018).

Tachyzoites (Figure 2) are the stage that rapidly multiplied during the acute infections and, therefore, they will receive the immune response of the host. Besides, they will be transported through the host to become bradyzoites, the slow multiplication forms of the parasite observed in chronic infections that will result in the formation of cysts, avoiding the immune response of the host. (Figure 3) (Kochanoowsky and Koshy, 2018).

Cysts can be observed in the brain (main organ where the parasite settles), cardiac muscle and skeletal muscle (Kochanoowsky and Koshy, 2018).

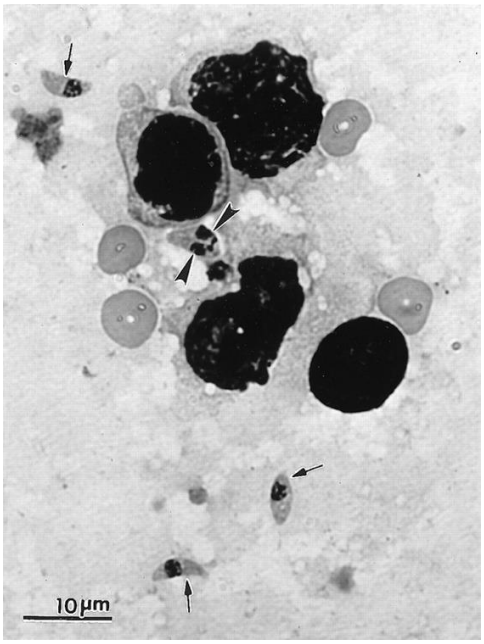

Figure 2. Dividing (arrowhead) and single (arrows) tachyzoites of *T. gondii.* Dubey, J.P., Lindsay, D.S., Speer, S.A. (1998). *Structures of Toxoplasma gondii, Tachyzoites, Bradyzoites, and Sporozoites and Biology and Development of Tissue Cysts.*

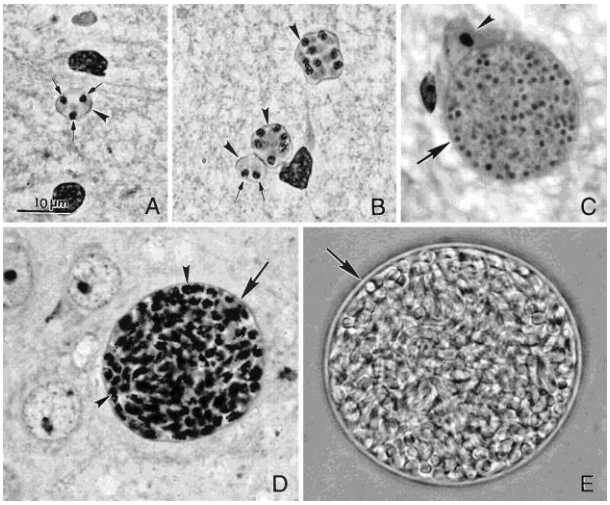

Figure 3. (A) *T. gondii* cyst with three bradyzoites inside (B). Three *T. gondii* cysts with two bradyzoites (arrows). (C), (D) and (E) *T. gondii* cysts with multiple bradyzoites inside. *Dubey, J.P., Lindsay, D.S., Speer, S.A. (1998). Structures of Toxoplasma gondii, Tachyzoites, Bradyzoites, and Sporozoites and Biology and Development of Tissue Cysts.*

1.1.1.2. Symptomatology

In both humans and animals, when a good immune response develops, the parasite usually affects asymptomatically or in a mild flu-like manner (Kochanoowsky and Koshy, 2018). However, symptomatic disease can be related to the tropism of the parasite and its persistence in the brain, and it usually occurs in immunocompromised individuals *(Liu et al., 2015).*

The most known and studied strains are called type I, II and III (haplotypes 1, 2 and 3), whose acute virulence in mice would be, type I strains lethal, type II strains moderately lethal and type III strains present little lethality (Kochanoowsky and Koshy, 2018).

Therefore, the pathogenicity of *T. gondii* is determined by host susceptibility, strain virulence and parasite stage *(Liu et al., 2015).*

1.1.1.3. Acting at brain level

Toxoplasma gondii likely reaches the brain via the vascular route, resulting in immunosuppressed patients, behavioral problems, such as reduced urine avoidance in cats or reduced anxiety, which could be due to specific cyst-infected neurons, brain inflammation, and/or changes in hormone levels (Kochanoowsky and Koshy, 2018).

1.1.1.4. Diagnostic methods

Oocysts present in the feces of infected cats, in contaminated water, in the environment or even tachyzoites present in tissues, can be detected thanks to concentration methods or microscopically by direct smear *(Liu et al., 2015)* or staining with Giemsa or PAS (Dubey, 2004).

As best measures for its detection, we find the isolation of *T. gondii* in laboratory animals by bioassay, by serological methods such as ELISA, dye test (DT), indirect fluorescent antibody test (IFAT), etc., for the demonstration of antibodies against the parasite.

In addition, imaging tests such as Computed Tomography (TC) scan for initial detection and Magnetic Resonance Imaging (MRI) may be performed to determine the extent of the lesion.

Among all of them, amplification tests are also performed for the detection of parasite DNA *(Liu et al., 2015).*

1.1.1.5. Preventive measures

Persons handling meat should adequately wash their hands with soap and water before and after handling meat. In addition, any material that has been in contact with the meat should also be properly washed. This should also be considered for vegetables before consumption.

The parasite present in meat dies when exposed to extreme cold or heat. For example, tissue cysts will die at an internal temperature of 67 degrees or 13 degrees. Therefore, meat should be warmed to that temperature before consumption.

Drinking unfiltered water from rivers or ponds should be avoided, as well as cats' access to water tanks (Dubey, 2004).

1.1.2. *Toxoplasma gondii* in marine mammals

The first detected case of toxoplasmosis in cetaceans was described in Brazil, in a coastal dolphin (*Sotalia guianensis*) (Bandoli and Oliveira, 1977). Subsequently, more cases have been detected in Europe, America and the Caribbean (Table 1) (*Van bressem et al., 2009, Dubey et al., 2020).* It is believed to be an opportunistic pathogen in marine mammals (*Migaki et al., 1990*). Risk factors for toxoplasmosis in cetaceans may include coinfection with Cetacean Morbillivirus (CeMV) (*Di Guardo et al., 2013*), as in the case of striped dolphins (*Stenella coeruleoalba)* during the first CeMV epidemic. in the Mediterranean Sea between 1990 and 1992 (*Domingo et al., 1992; Kennedy, 1998*), but also a low genetic

diversity (*Roe et al., 2013*) and a coastal habitat (*Bowater et al., 2003*). Nevertheless, (*Di Guardo et al., 2010*) points out the role of this protozoan as the primary and unique agent in the development of non-suppurative meningoencephalitis in striped dolphins stranded on the Italian coast (*Di Guardo et al., 2010*).

The way in which marine mammals become infected is thought to be due to contamination of the aquatic environment and therefore transport of oocysts via water currents or even some animals becoming infected by ingestion of fish *(Dubey et al., 2020).* In addition, migratory filter-feeding fish such as northern anchovies (*Engraulis mordax*) and Pacific sardines (*Sardinops sagax*) are thought to act as vectors of *T. gondii* from the coast to the ocean (*Massie et al., 2010).* Alternatively, infection can also occur via the transplacental route (*Van Bressem et al., 2009*). In a study conducted in Hawaii between 2001 and 2015 of 183 monk seals, *T. gondii* was found in 8 of them, one of the cases being a stillborn foetus with the parasite present in the lung, umbilical cord and placenta, which was part of the first reported placental transmission of *T. gondii* in a monk seal *(Dubey et al., 2020).*

It has been shown that otters whose diet is based on a higher proportion of marine snails than other mollusks have a higher seroprevalence against the parasite. This could be explained by the fact that snails absorb *T. gondii* oocysts and become carriers for 10 days and can shed the parasite in their faeces. In addition, the location and habitat of the otter also influences the presentation of the parasite *(Dubey et al., 2020).*

In general, the clinical signs and lesions produced by *T. gondii* in marine mammals are lymphadenitis, necrotic adrenalitis, myocarditis, abortions, acute interstitial pneumonia, non-suppurative encephalitis and systemic disease (*Van Bressem et al., 2009).*

Table 1. Marine mammal species with positive *T. gondii* seroprevalence between 2009 and 2020. (*Dubey et al., 2020).*

DOLPHINS	
Atlantic Bottlenose dolphin (*Tursiops truncatus truncatus*)	Canada, Europe - Atlantic Ocean, North Sea, Italy, Mexico, Spain – Valencia, USA – Florida, South Carolina
Black Sea Bottlenose dolphin (*Tursiops truncatus ponticus*)	Russia
Pacific Bottlenose dolphin	Mexico

(*Tursiops truncatus gillii)*	
Atlantic white-sided dolphin (*Lagenorhynchus acutus*)	Europe - Atlantic Ocean, North Sea
Fraser's dolphin (*Lagenodelphis hosei*)	Philippines
Pantropical spotted dolphin (*Stenella attenuata*)	Philippines
Risso's dolphin (*Grampus griseus*)	Europe - Atlantic Ocean, North Sea
Striped dolphin (*Stenella coeruleoalba*)	Europe - Atlantic Ocean, North Sea, Italy
White-beaked dolphin (*Lagenorhynchus albirostris*)	Europe - Atlantic Ocean, North Sea
Short-beaked common dolphin (*Delphinus delphis*)	United Kingdom, Europe - Atlantic Ocean, North Sea
DUGONGS	
Dugong dugon	Australia
MANATEE	
Amazonian manatee (*Trichechus inunguis*)	Brazil, Peru
Antillean manatee (*Trichechus manatus manatus*)	Belize, Brazil, Puerto Rico
Florida manatee (*Trichechus manatus latirostris*)	USA - Florida
OTTERS	
Eurasian otter *(Lutra lutra*)	United Kingdom
Marine otter (*Lontra felina*)	Chile
Southern sea otter (*Enhydra lutris nereis*)	Europe - North Sea, USA - California
Northern sea otter (*Enhydra lutris kenyoni*)	Russia, USA - Washington
PORPOISE	
Harbour porpoise (*Phocoena phocoena*)	Europe - Atlantic Ocean, North Sea, United Kingdom
SEA LION	
California sea lion (*Zalophus californianus*)	Mexico, USA - California
New Zealand sea lion (*Phocarctos hookeri*)	New Zealand – Sub-Antarctic
SEALS	
Antarctic fur seal (*Arctocephalus gazella*)	Antarctica
Atlantic harbor seal *(Phoca vitulina vitulina*)	Canada, Europe - Atlantic Ocean, North Sea,

	France, Scotland – Atlantic coasts
Harbour seal (*Phoca vitulina*)	Norway – Svalbard, USA – Alaska, USA - California
Australian fur seals (*Arctocephalus pusillus doriferus*)	Australia
Bearded seals (*Erignathus barbatus*)	Canada, Norway
Caspian seals (*Pusa caspica*)	Iran - Northern
Crabeater seal (*Lobodon carcinophaga*)	Antarctica
Grey seal (*Halichoerus grypus*)	Europe - Atlantic Ocean, North Sea, France, Scotland – Atlantic coasts
Ringed seal (*Pusa hispida*)	Canada, Norway
Southern elephant seal (*Mirounga leonina*)	Antarctica
Weddell seal (*Leptonychotes weddellii*)	Antarctica
WALRUS	
Walrus (*Odobenus rosmarus*)	Canada
WHALES	
Beluga whale (*Delphinapterus leucas*)	Canada, Norway, Russia
Pygmy killer whale (*Feresa attenuata*)	Philippines
Bowhead whale (*Balaena mysticetus*)	Canada
Humpback whale (*Megaptera novaeangliae*)	United Kingdom – England, Wales
Whales spp.	Europe - Atlantic Ocean, North Sea

1.1.3. Toxoplasmosis in stranded cetaceans in the Canary Islands

Two Atlantic spotted dolphins (*Stenella frontalis*), out of the 233 cetaceans (0.9%) (90 Delphinidae) stranded and subjected to morphopathological studies in a study conducted between 1999 and 2005 in stranded cetaceans in the Canary Islands, were found to have encephalitis caused by *T. gondii (Arbelo et al., 2013)*; while in the study conducted between 2006 and 2012, disseminated toxoplasmosis (Figure 4) was diagnosed in six Atlantic spotted

dolphins, including four adult males, one adult female and one calf female, out of 224 cetaceans from which a postmortem examination was conducted (2.7%) *(Diaz-Delgado et al., 2018)*. No other cetacean species was diagnosed of toxoplasmosis in those years in this geographical area.

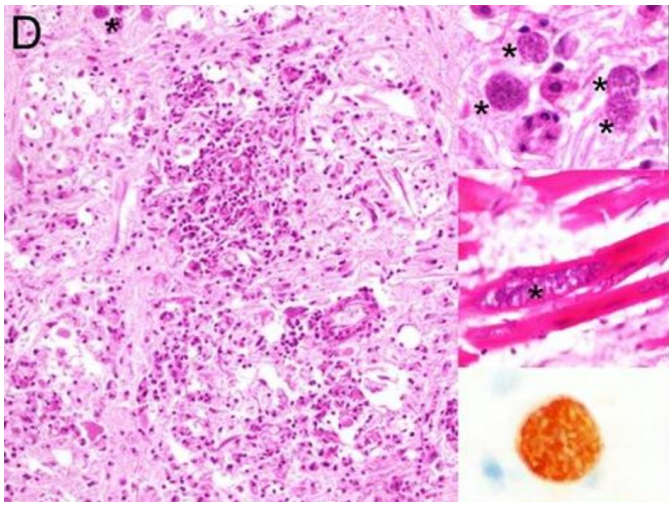

Figure 4. The third image on the right down shows the presence of a brain cyst positive for *T. gondii* antibodies in the immunohistochemical test. In the second image on the right in the middle, cysts of the parasite are also present in the sarcoplasm of cardiomyocytes. While in the first image on the right up, cysts without inflammation are observed. In the remaining image on the left, inflammation of the white matter is observed with the presence of necrosis and decreased density of the neuroparenchyma, in addition, the asterisk refers to the presence of a parasite cyst *(Diaz-Delgado et al., 2018).*

2. OBJECTIVES

The main objectives of this study are:

- To determine the prevalence of the protozoan *Toxoplasma gondii* in striped dolphins stranded on the coasts of the Canary Islands.
- To describe the lesions caused by this protozoan in these stranded striped dolphins.

3. MATERIAL AND METHODS

The animals included in this study were cetaceans stranded in the Canary Islands between 2000 and 2022 (n = 1183). The information about each stranding (date, location with coordinates and type) and decomposition stage (grade 1: extremely fresh carcass; grade 2: fresh carcass; grade 3: moderate decomposition; grade 4: advanced decomposition and grade 5: mummified or skeletal remains) was systematically recorded, as well as life history data (species, age category, sex and body condition). The nutritional status was classified as good,

moderate, poor or emaciated in consonance with anatomical parameters, the observable presence of dorso-axial muscular mass and the presence or distribution of fatty tissue in several organs, taking into consideration the species and the age of the animals. Two hundred and seventeen out the total of recorded strandings in this period (18.3%) involved striped dolphins (*Stenella coeruleoalba*), from which a complete pathological study was performed in 168 (77.4%). All the cases included in the present study were diagnosed during routine pathological and cause-of-death analyses in stranded cetaceans at the Division of Histology and Animal Pathology of the Institute for Animal Health (IUSA), Veterinary School, Universidad de Las Palmas de Gran Canaria. As a result, lesions associated with the presence of tissue cysts compatible with *T. gondii* in different anatomic locations were detected in two male striped dolphins stranded in Tenerife in 2021 and 2022 (animal number 1 and animal number 2, respectively).

Animal number 1 was found swimming alive near the shore in a poor body condition, dying before being attended. It was an adult in a very fresh condition (conservation grade 1) (Figure 5). Animal number 2 was found stranded dead with a very poor body condition. It was a subadult in a fresh condition (conservation grade 2) (Figure 6).

Figure 5. Right lateral view of animal number 1.

Figure 6. Left dorso lateral view of animal number 2.

These two animals were examined and necropsied according to standard procedures (*Kuiken and García Hartmann, 1993; Isseljdik, Brownlow and Mazzariol, 2019*). During necropsy, all tissues and organs, after being correctly examined and dissected, were sampled (Supplemental material table 1) and preserved in buffered 10% formalin for histopathology. Additionally, samples of selected organs were taken and frozen at -80ºC for molecular diagnosis tests.

Samples were fixed in 10% formalin, embedded in paraffin, sectioned at 5µm, and stained with hematoxylin and eosin (H&E) for examination by light microscopy.

Molecular detection of *T. gondii* was carried out by a real-time PCR amplifying a 163 bp sequence within the *T. gondii* small subunit ribosomal RNA (18SrRNA), as previously described (*Sierra et al., 2020*) in a subset of samples: adrenal gland, brain, heart, lung, and rete mirabile in animal number 1; and adrenal gland, brain, heart, liver, lung, and rete mirabile in animal number 2. Previous extraction of DNA/RNA was carried out by pressure followed afiltration method, using a QuickGene R Mini 80 nucleid acid isolation instrument, using the DNA Tissue Kit S (QuickGene, Kurabo, Japan) according to the manufacturer's instructions with modifications: RNA carrier (Applied BiosystemsTM, Thermo Fisher Scientific Waltham, Massachusetts, USA.) was added during the lysis step (*Sacristán et al., 2015*).

The same samples were also tested for Cetacean Morbillivirus (CeMV) by a real PAN RT-qPCR method based on SYBRN® green dye that successfully detects GDMV, PWMV and DMV strains. The primer set amplifies 205 bp from a region of the phosphoprotein (P) gene (*Groch et al., 2020*).

4. RESULTS

In this section, we summarize the most significant lesions, both macroscopic and microscopic, present in both animals (the rest of the observed changes can be found in Annex 2).

- **Animal number 1:**

Morphologically, the animal presented a moderate to severe multiorgan necrosis and lymphohistiocytic inflammation with intralesional protozoa (CNS, heart, skeletal muscle, adrenal glands, pancreas, liver, lung, rete mirabile, spleen, pituitary gland) (Figures 7-15). In the lung, we can see a moderate-severe chronic lymphoplasmacytic interstitial bronchopneumonia; and in the lymphoid organs, a moderate multinodal follicular depletion, and moderate reactive lymphoid hyperplasia of the laryngeal and pharyngeal tonsils.

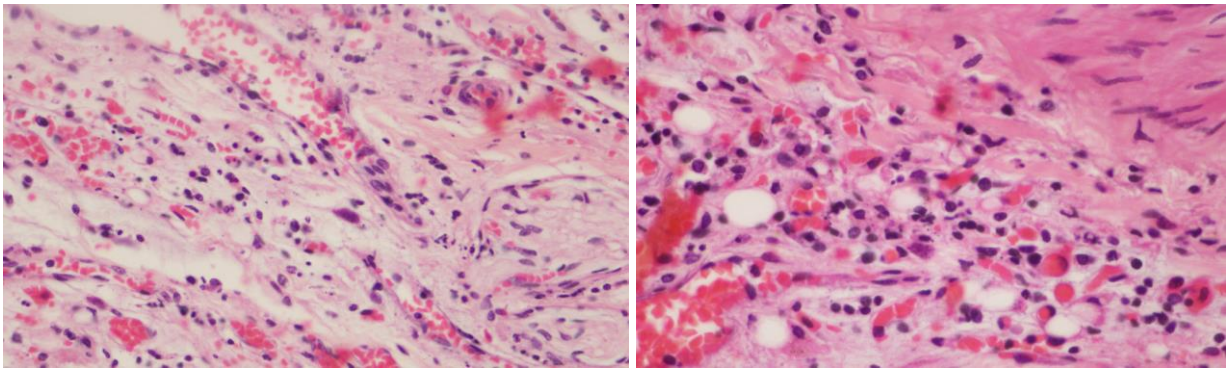

Figure 7. Rete mirabile. Left: Mild lymphohystiocitic inflammation with a tissue cyst. H&E, 4x. **Right:** closer view of a similar lesion with an associated tissue ctyst. H&E, 10x.

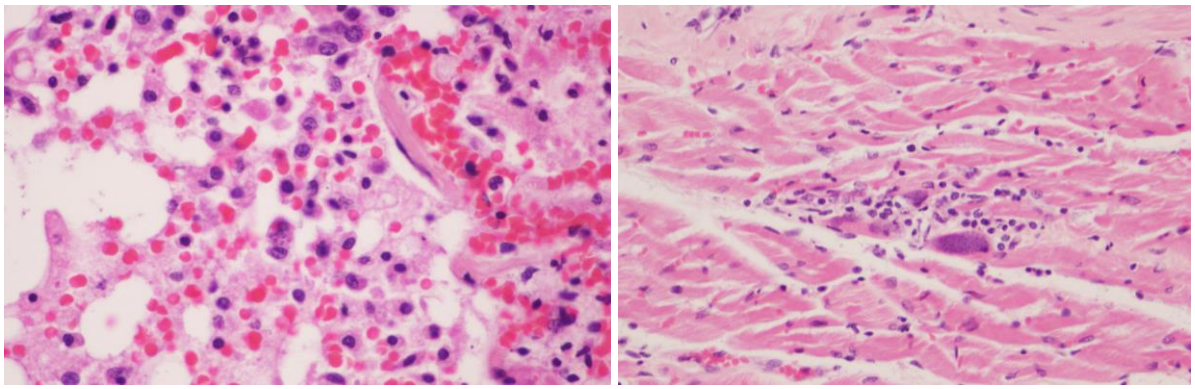

Figure 8. Left: Lung, alveolar haemorrhage intermixed with scattered lymphohistiocytic inflammatory cells and intracellular tachyzoites. H&E, 20x. **Right:** Heart. A tissue cyst in a cardiomyocyte associated with infiltration of macrophages and lymphocytes. H&E, 4x.

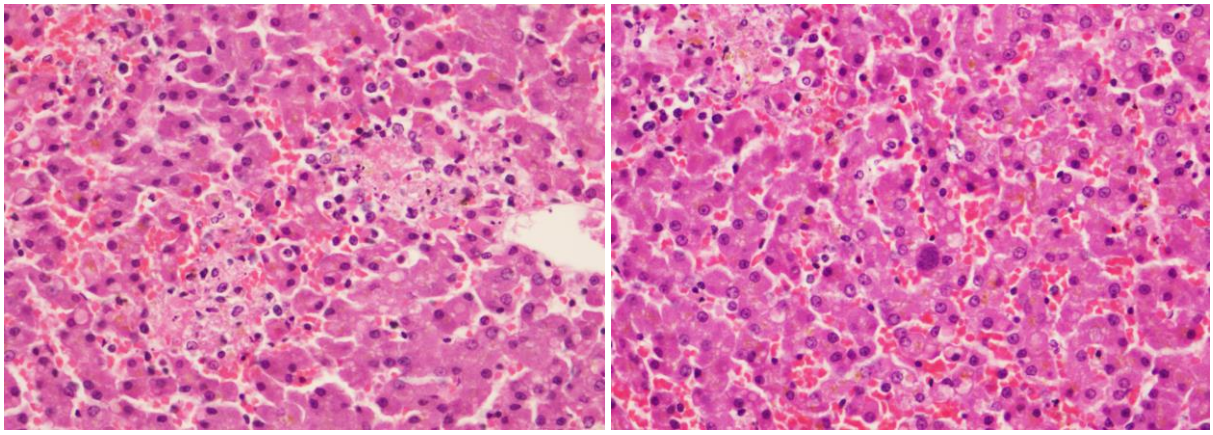

Figure 9. Liver. Left: Moderate granulomatous and lymphocytic to necrotizing hepatitis. H&E, 10x. **Right:** many small, randomly distributed, necrotic foci containing mononuclear leukocytic infiltrates with *T. gondii* organisms occasionally found in hepatocytes. H&E, 10x.

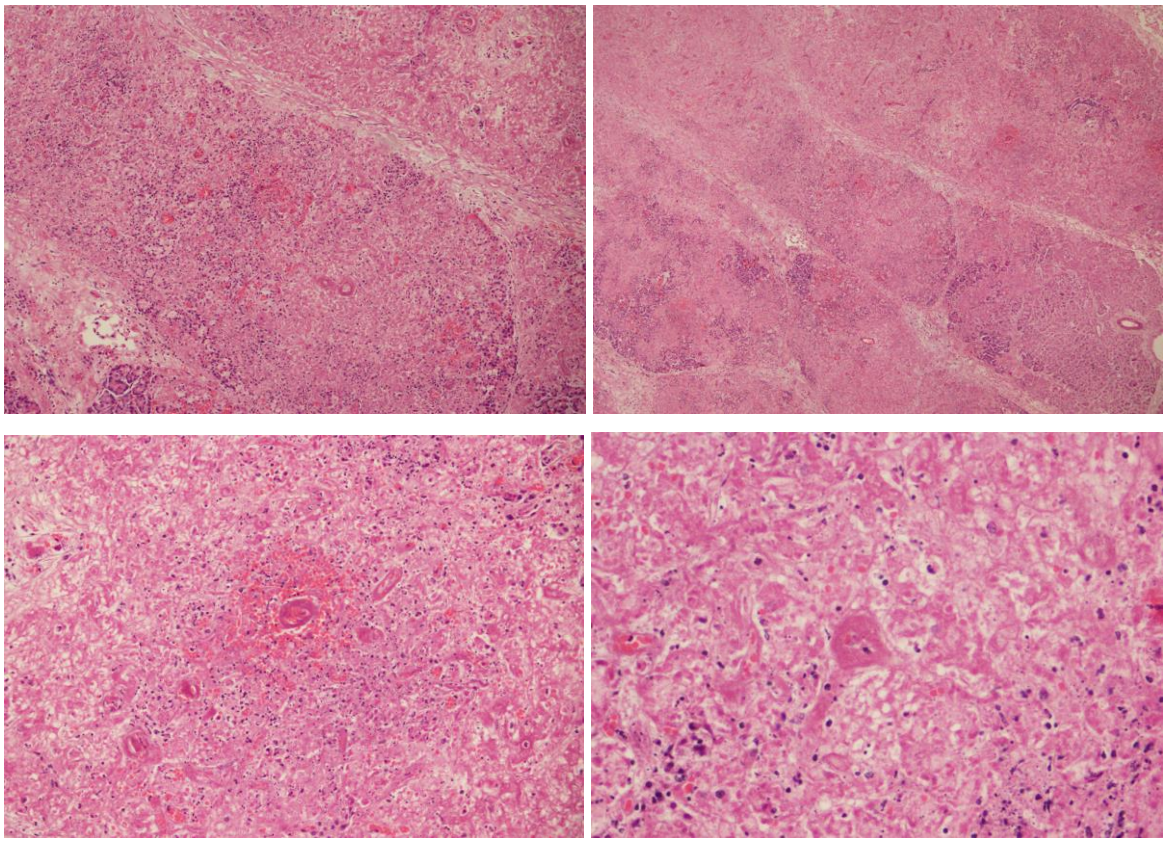

Figure 10. Pancreas. Severe extensive coagulative necrosis of the pancreas. Up left: H&E, 4x. **Up right:** H&E, 4x. **Down left:** Intravascular coagulation and associated parenchymal haemorrhages and coagulative necrosis. H&E, 10x. **Down right:** Detail of intravascular coagulation and parenchymal coagulative necrosis. H&E, 20x.

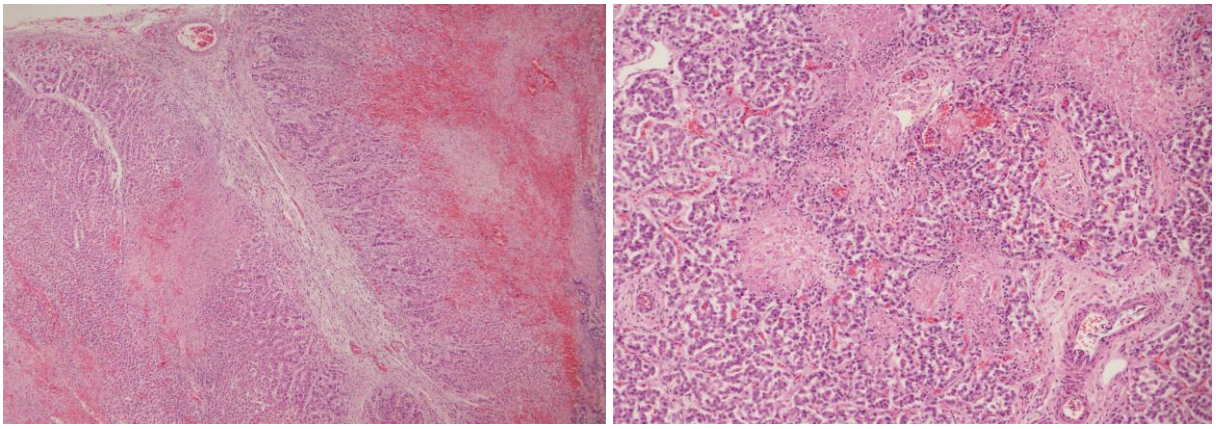

Figure 11. Severe and extensive coagulative necrosis in the adrenal gland. Left: multiple foci in the cortex with associated haemorrhages. H&E, 4x. **Right:** fewer lesions were found in the medulla. H&E, 10x.

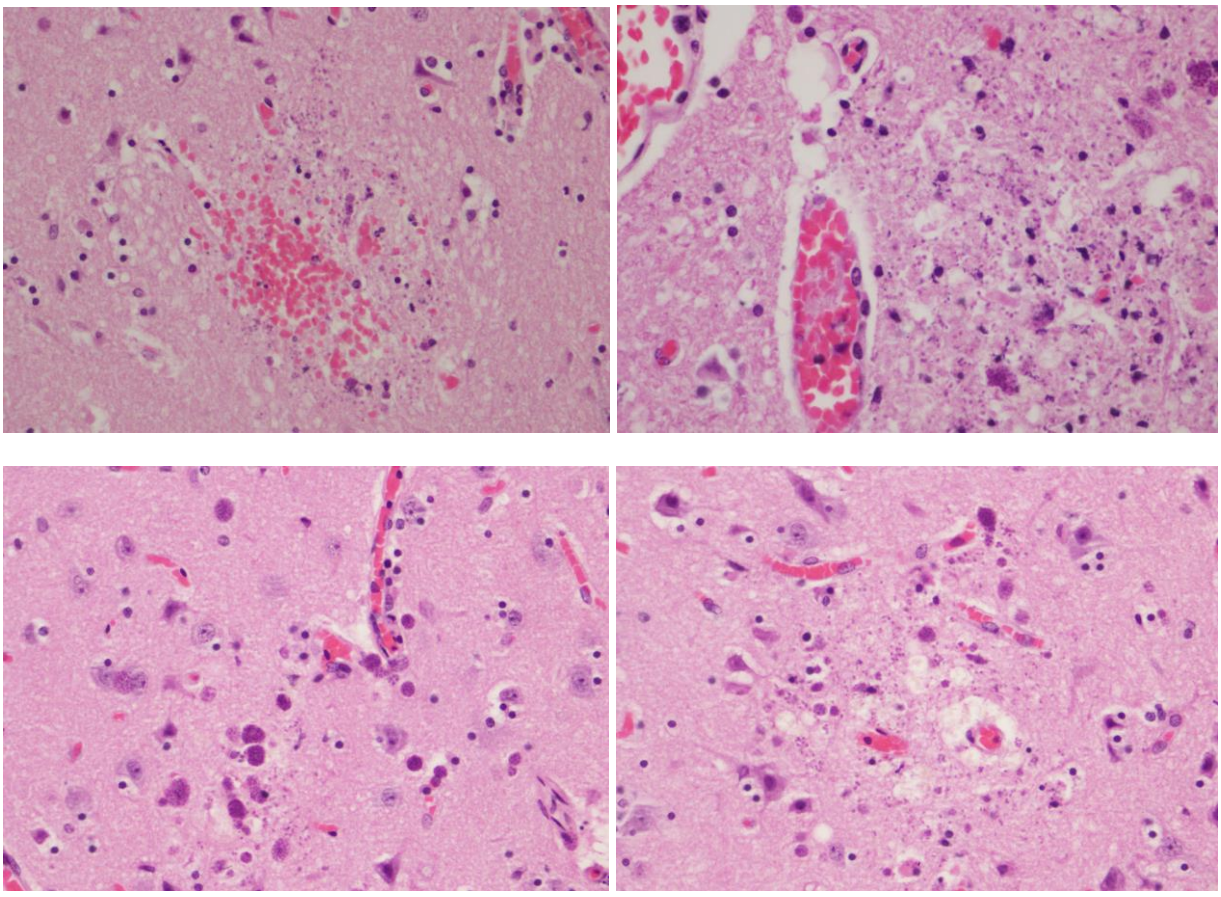

Figure 12. CNS. Up Right: Haemorrhages and necrosis of the neuropil. H&E, 10x. **Up Left:** Focal necrosis with associated degenerating tachyzoites and tissue cysts. H&E, 20x. **Down Left:** Perivascular tachyzoites and tissue cysts. H&E, 40x. **Down Right:** acute degenerative changes in the neuropil associated to the presence of tachyzoites. H&E, 40x.

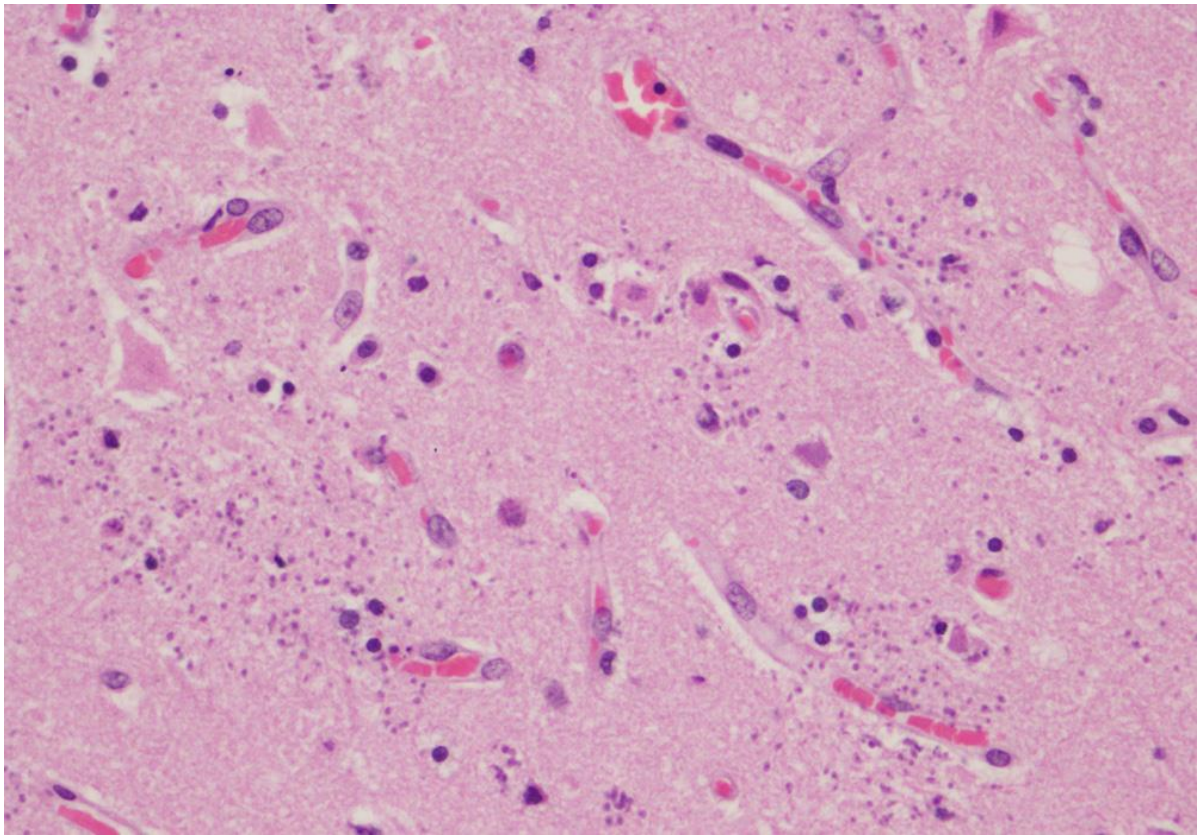

Figure 13. CNS. Acute intravascular dissemination to the CNS of large amounts of tachyzoites. H&E, 60x.

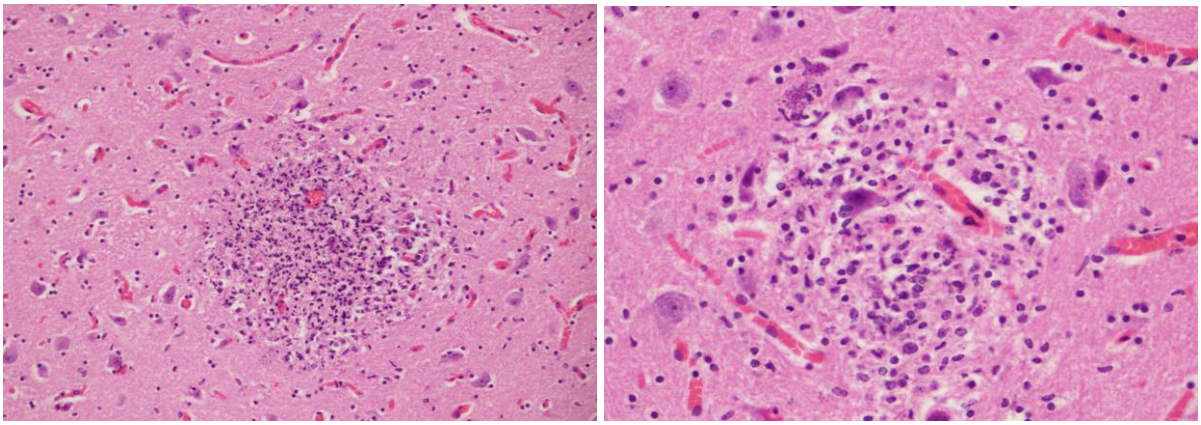

Figure 14. CNS. Nonsuppurative necrotizing encephalitis were associated with degenerating tachyzoites. **Left:** H&E, 20x. **Right:** H&E, 40x.

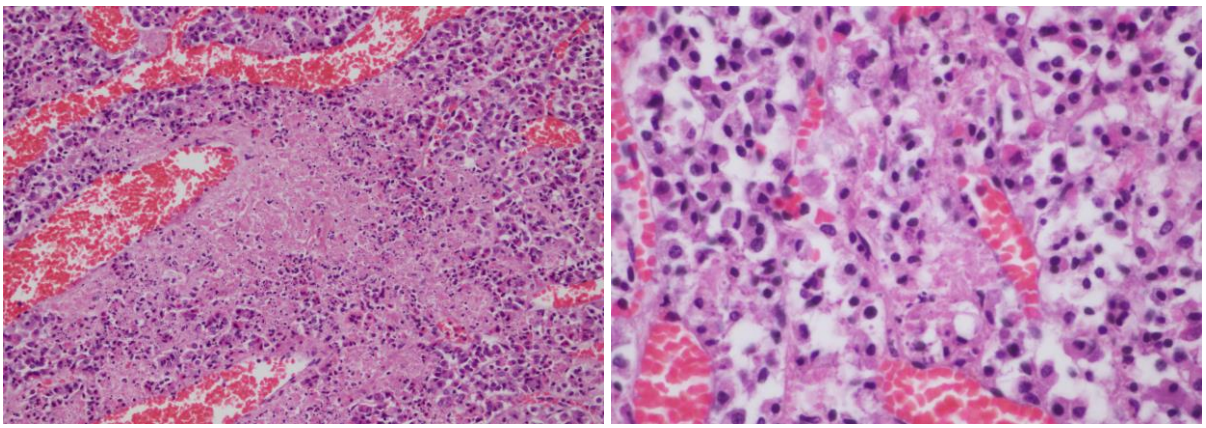

Figure 15. Adenohypophysis. Left: Focally extensive coagulative necrosis. H&E, 20x. **Right:** focal necrosis with admixed tachyzoites. H&E, 40x.

In terms of aetiology, microscopic lesions compatible with systemic toxoplasmosis were observed, including necrotizing lesions with intracellular protozoan cysts and intralesional extracellular zooites in various organs, with severe involvement of the CNS, adrenal glands, pancreas, and pituitary gland (Figure 16). Based on the lesions observed, it is concluded that the cause of the stranding and subsequent death was a disseminated infection by *Toxoplasma* sp.

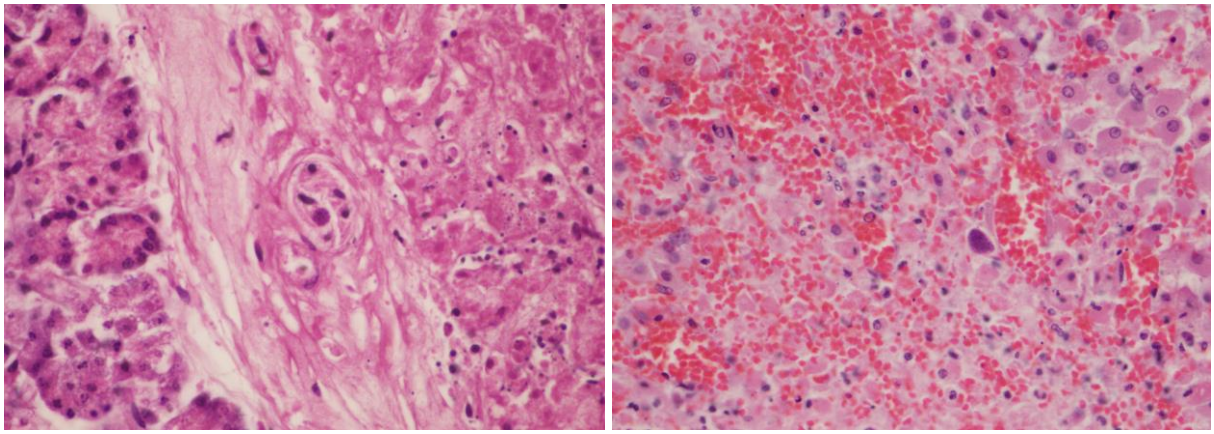

Figure 16. Left: Pancreas. Detail of a tissue cyst in a nerve ganglia and parenchymal coagulative necrosis. H&E, 20x. **Right: Adrenal gland.**

- **<u>Animal number 2:</u>**

Morphologically, the animal presented a moderate to severe multiorgan necrosis and lymphohistiocytic inflammation with intralesional protozoa (CNS, heart, vascular system, digestive tract, bladder, prostate, adrenal glands, thyroid). Severe necrosis in the adenohypophysis. In the lymphoid organs there were a severe multinodal follicular depletion (Figure 17).

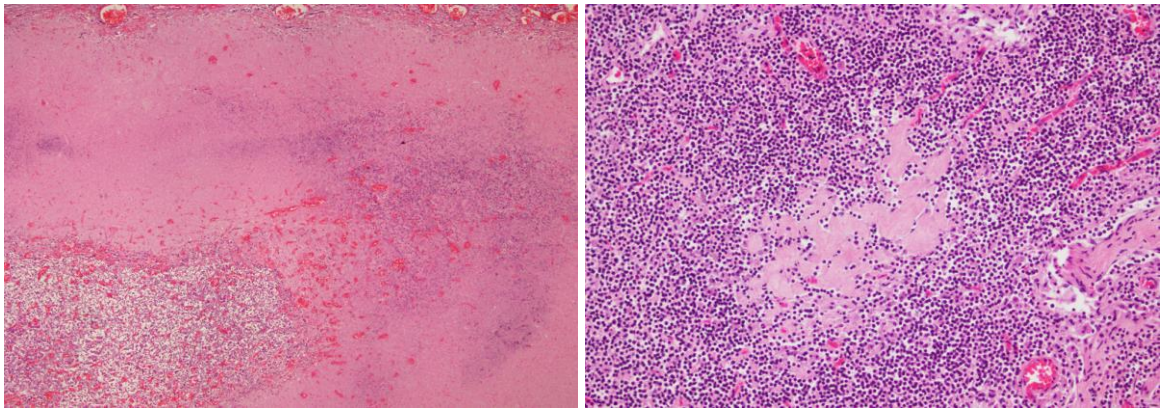

Figure 17. Left: Adenohypophysis. Severe extensive coagulative necrosis. H&E, 4x. **Right: Lymph node.** Follicular hyalinosis in the center of depleted follicles. H&E, 20x.

Other findings included: focal ulcerative glossitis, focal ulcerative gastritis and multiorgan parasitosis. Fractures of the mandible and left tympanic-periotic complex and hemorrhages of surrounding soft tissues were also found.

In terms of aetiology, microscopic lesions compatible with systemic toxoplasmosis were observed, including necrotizing lesions with intracellular protozoan cysts and intralesional extracellular zoites in various organs, with severe involvement of the central nervous system (Figures 18-20). In addition, the animal presented bilateral fractures of the shaft of the mandible and periotic tympanic complex on the left side, with hemorrhages in the surrounding soft tissues, possibly caused by a prior death trauma of unknown origin. Based on the lesions observed, it is concluded that the cause of death in this individual was associated with disseminated infection by *Toxoplasma* sp., although the possible presence of other infectious agents is not ruled out. Complementary studies (histochemical, microbiological and/or molecular) are recommended to confirm the possible etiological agents responsible for the pathological process.

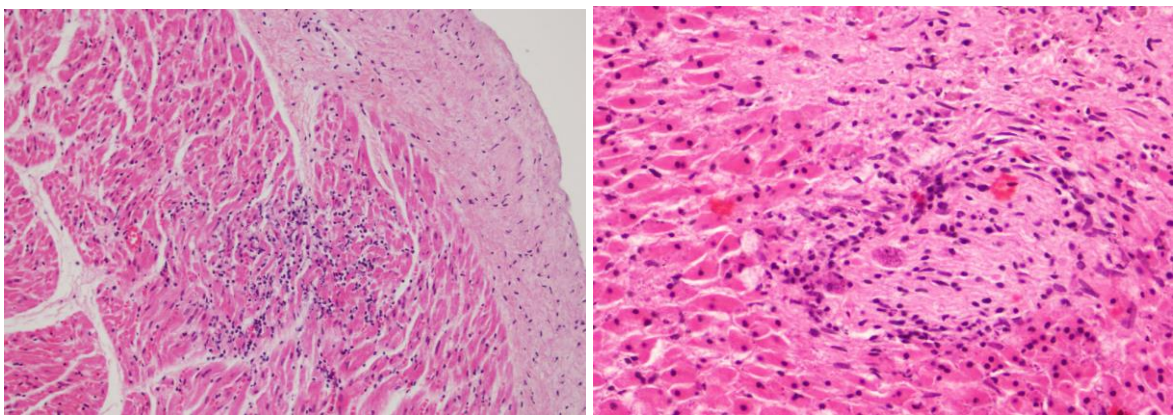

Figure 18. Left: Heart: Myocardium showing multifocal mild to moderate infiltration of macrophages and lymphocytes. H&E, 10x. **Left: Adrenal gland.** A tissue cyst in a nerve ganglia associated with lymphohystiocytic inflammation. H&E, 20x.

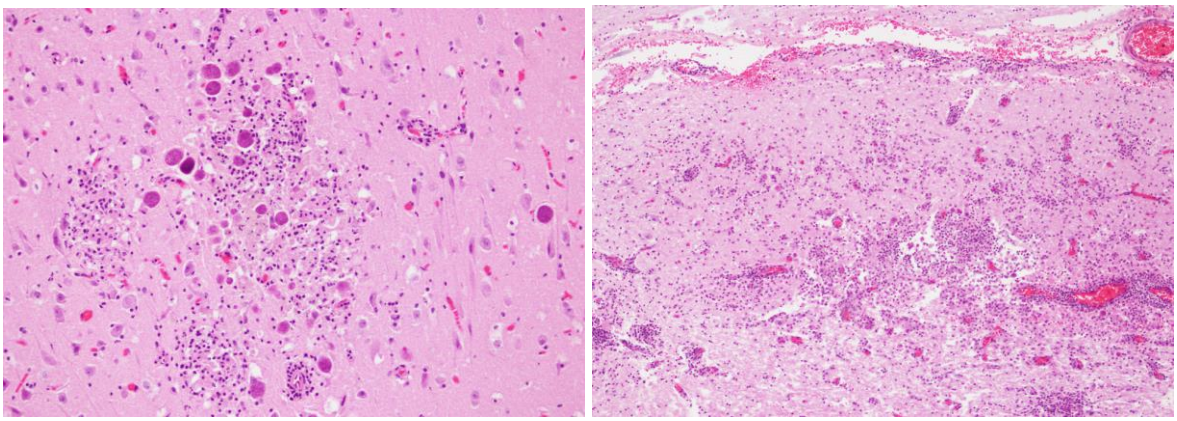

Figure 19. CNS. Left: Tissue cysts with associated non-suppurative encephalitis. H&E, 10x. **Right:** Perivascular cuffing and multiple foci of non-suppurative encephalitis. H&E, 4x.

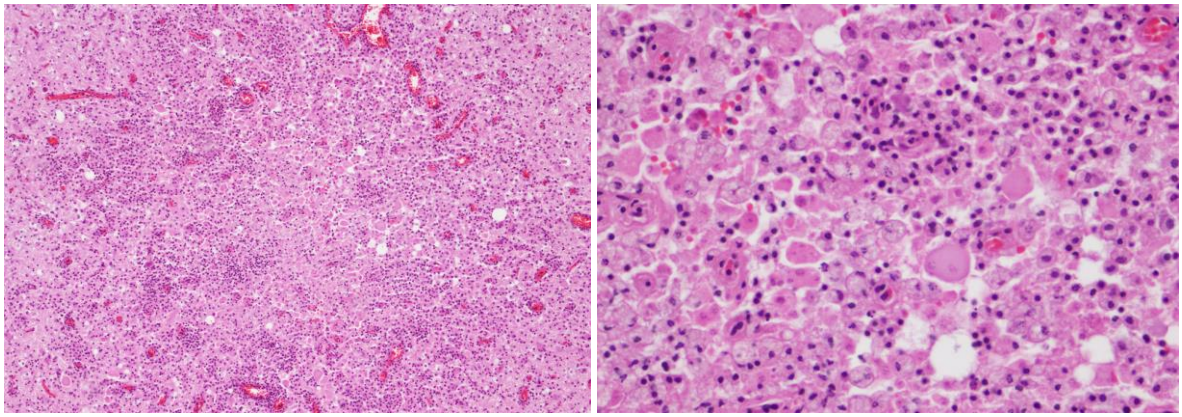

Figure 20. CNS. Left: Severe granulomatous and lymphohistiocytic inflammation with multinucleated giant cells. H&E, 20x. **Right:** higher magnification of the inflammatory foci. H&E, 60x.

All the tested samples, except the liver sample from animal number 1 resulted positive for *T. gondii* and negative for CeMV.

5. DISCUSSION

The presence of *T. gondii* in cetaceans, more specifically within the family Delphinidae, has been the subject of very few studies due to the low presence of the parasite in these animals. However, in the recent years, there has been a growing interest based on the increased presence of the parasite in cetaceans, which could be indicative of a widespread contamination of marine waters with the infecting oocysts (*Dubey et al., 2020*).

We report toxoplasmosis in two striped dolphins stranded in the Canary Islands, where there was no previous description of the disease in this species, in contrast to the Atlantic spotted dolphin species, from which lesions associated to the presence of *Toxoplasma* had been detected in 8 animals (*Arbelo et al., 2013, Díaz-Delgado et al., 2018*).

The prevalence of the infection for the 23-year period of study in the archipelago is 5.12% for the Atlantic spotted dolphin (8 positive animals out to 156 stranded animals with a complete anatomopathological study) and 1.2% for the striped dolphin. However, for pelagic cetacean species, such as the striped dolphin, reports of toxoplasmosis in other geographical areas, such as the Mediterranean Sea, are common (*Domingo et al., 1992, Kennedy et al., 1998 Di Guardo et al., 2010*).

A 1990 study on the presence of *T. gondii* in a spinner dolphin (*Stenella longirostris*) in Hawaii concluded that cetaceans can contract fatal diseases from the parasite (*Migaki et al., 1990*). The histopathological description in that case included: numerous large, discrete areas of coagulative necrosis in the cortex (with fewer lesions in the medulla) of the adrenal gland, with mononuclear leukocytic aggregates (mainly composed of lymphocytes and macrophages) at the periphery of the necrotic areas and intralesional numerous organisms of *T. gondii*, including both tachyzoites and tissue cysts (*Migaki et al., 1990*). A diffuse encephalitis was present with numerous small foci of gliosis associated with tissue cysts. The liver had many small, randomly distributed, necrotic foci containing mononuclear leukocytic infiltrates, and *T. gondii* organisms were found occasionally in hepatocytes. A severe subacute to chronic suppurative bronchopneumonia, with multiple large areas of necrosis, was attributed to *Aeromonas* sp. and *Pseudomonas putrefaciens*, since no *Toxoplasma* organisms were found in the lung.

Since them, the main lesions described in cetacean cases of toxoplasmosis are in accordance with this first description and include: necrotizing hepatitis, lymphadenitis and lymphoid necrosis, interstitial pneumonia, adrenal necrosis, and non-suppurative encephalitis and meningoencephalitis with bradyzoites and free tachyzoites; although the protozoans can be found in almost all tissues, generally in close association with necrotizing and mainly non- suppurative inflammatory lesions (*Inskeep et al., 1990, Mikaelian et al., 2000, Resendes et al., 2002, Van Bressem et al., 2009, Gonzales-Viera et al., 2013, Roe et al., 2013, Herder et al., 2015, Costa Silva et al., 2019*). However, it has been suggested that the acquired immunity is sufficient to suppress infection in some

organs but not in others where a higher immunity level is necessary, like the adrenals, the brain, and the liver (*Frenkel 1998*).

In our study, the two animals displayed similar lesions associated to the protozoan, highlighting the severe involvement of the central nervous system, as previously described (*Di Guardo et al., 2010, Sierra et al., 2020, Morell et al., 2021*). However, we have not found any previous description of severe necrotic lesions in organs such as the pancreas (animal number 1) and the hypophysis (animal number 1 and number 2) as it was observed in our study and in one calf of the Atlantic spotted dolphin species stranded in the Canary Islands in 2009. Reported cases of toxoplasmosis infection involving the pituitary gland are unusual, with only few human cases (*Milligan et al., 1984, Zhang et al., 2002, Prayson et al., 2017*).

In *T. gondii*-positive cases from our study, all tested tissues were negative for morbillivirus, suggesting that *T. gondii* possibly acted as a primary agent, as previously observed (*Di Guardo et al., 2010, Gonzales-Viera et al., 2013, Roe et al., 2013*). Nevertheless, some histopathologic findings such as lymphoid depletion and necrotizing stomatitis, compatible with opportunistic bacterial or viral infections (or both) (*Jones et al., 1997, Resendes et al., 2002*), could suggest that these animals were most likely immunosuppressed.

Most of the knowledge of the *T. gondii* infection consequences in cetaceans is known from research on southern otters (*Enhydra lutris*), which live in areas of high freshwater runoff, as a major cause of mortality (*Massie et al., 2010*) and encephalitis (*Dubey et al., 2003*). After ingestion, bradyzoites from the tissue cysts or sporozoites from the oocysts penetrate the intestinal epithelial cells and multiply in the intestine. Then, *T. gondii* may spread first to mesenteric lymph nodes and then to distant organs by the invasion of lymphatics and blood where intracellular growth of tachyzoites causes necrosis (*Dubey et al., 1998*).

In our study, *T. gondii* tachyzoites were observed, free or intracytoplasmatic, entering or exiting directly from the blood vessels, indicating that the parasite spreads through the host both freely and attached to host immune cells, which is known as the Trojan horse hypothesis, where leukocytes, macrophages, neutrophils and monocytes are of particular importance as they contribute to parasite dissemination due to their ability to infect these cells (Weidner and Barragán, 2014).

Further studies are warranted to characterize the circulating strains in the Canary waters and to clarify the distribution of this protozoan, its transmission route(s), unsolved pathogenetic mechanisms, cetacean host-specific susceptibilities, and potential implications to the conservation of cetacean species of the archipelago and mechanisms involved in human exposure.

6. CONCLUSION

The presence of *T gondii* tachyzoites and tissue cysts in several organs (confirmed by PCR) of the two animals and the absence of concurrent morbillivirus infection support the hypothesis that this protozoan played a primary etiologic role in the development of the observed severe lesions.

Despite the low incidence of toxoplasmosis in striped dolphins stranded in the Canary Islands compared with proximal geographical areas, such as the Mediterranean Sea, the results of this study widen the geographic range of this agent for one of the most *T. gondii*-susceptible species, the striped dolphin.

The extensive distribution of the lesions in the adrenal glands, pancreas, hypophysis, liver, and brain is consistent with a prolonged primary infection rather than related to a reactivation of preexisting latent *Toxoplasma* infection.

7. BIBLIOGRAPHY

- Arbelo, M., Espinosa de los Monteros, A., Herráez, P., Andrada, M., Sierra, E., Rodríguez, F., Jepson, P.D., Fernández, A. (2013). Pathology and causes of death of stranded cetaceans in the Canary Islands (1999-2005). *Diseases of Aquatic Organisms, 103*, 87-99.
- Attias, M., Teixeira, D., Benchimol, M., Vommaro, R.C., Crepaldi, P.C., De Souza, W. (2020). The life-cycle of *Toxoplasma gondii* reviewed using animations. *Parasites and Vectors, 13*(1).
- Bandoli, J. G., Oliveira, C.A.B. (1977). Toxoplasmose em *Sotalia guianensis* (Van Beneden, 1863), Cetacea, Delphinidae. *Importância Médico-Social Folha Médica, 75*, 459-468.
- Bowater, R.O., Norton, J.A., Johnson, S.C., Hill, B.D., O'Donoghue, P.J., Prior, H. (2003). Toxoplasmosis in Indo-Pacific humpbacked dolphins (*Sousa chinensis*), from Queensland. *Australian Veterinary Jorunal, 81*(10), 627-632.
- Costa-Silva, S., Sacristán, C., Gonzales-Viera, O., Diáz-Delgado, J., Sánchez-Sarmiento, A.M., Marigo, J., Groch, K.R., Carvalho, V.L., Ewbank, A.C., Colosio, A.C., Marcondes, M.C.C., Meirelles, A.C.O., Bertozzi, C.P., Lailson-Brito, J., Azevedo, A.F., Ruoppolo, V., Oliveira, L., Ott, P.H., Catão-Dias, J.L. (2019). *Toxoplasma gondii* in cetaceans of Brazil: a histopathological and immunohistochemical survey. *Brazilian Journal of Veterinary Parasitology: Orgao Oficial do Colegio Brasileiro de Parasitologia Veterinaria, 28*(3), 395-402.
- Díaz-Delgado, J., Fernández, A., Sierra, E., Sacchini, S., Andrada, M., Vela, A.I., Quesada-Canales, O., Paz, Y., Zucca, D., Groch, K.R., Arbelo, M. (2018). Pathological findings and causes of death of stranded cetaceans in the Canary Islands (2006-2012). *PLOS ONE, 13*(10).
- Dierauf, L.A., Whitman, K.L., Gulland, F.M.D. CRC Handbook of Marine Mammal Medicine. Portland, USA: Taylor & Francis Inc; 2018.
- Di Guardo, G., Di Francesco. C.E., Cocumelli, C., Scholl, F., Casalone, C., Peletto, S., Mignone, W., Tittarelli, C.D., Di Nocera, F., Leonardi, L., Fernández, A.L., Marcer, F., Mazzariol, S. (2013). Morbillivirus infection in cetaceans stranded along the Italian coastline: Pathological, inmunohistochemical and biomolecular findings. *Research in Veterinary Science, 94*(1), 132-137.

- Di Guardo, G., Proietto, U., Di Francesco, C.E., Marsilio, F., Zaccaroni, A., Scaravelli, D., Mignone, W., Garibaldi, F., Kennedy, S., Forster, F., Iulini, B., Bozzetta, E., Casalone, C. (2010). Cerebral Toxoplasmosis in Striped Dolphins (*Stenella coeruleoalba*) Stranded Along the Ligurian Sea Coast of Italy. *Veterinary Pathology, 47*(2), 245-253.
- Domingo, M., Visa, J., Pumarola, M., Marco, A.J., Ferrer, L., Rabanal, R., Kennedy, S. (1992). Pathologic and inmunocytochemical studies of morbillivirus infection in striped dolphins (*Stenella coeruleoalba*). *Veterinary Pathology, 29*(1), 1-10.
- Dubey, J.P., Lindsay, D.S., & Speer, S.A. (1998). Structures of *Toxoplasma gondii*, Tachyzoites, Bradyzoites, and Sporozoites and Biology and Development of Tissue Cysts. *Clinical Microbiology Reviews, 11*(2), 267-299.
- Dubey, J.P., Murata, F.H., Cerqueira-Cézar, C.K., Kwok, O.C., Grigg, M.E. (2020). Recent epidemiological and clinical significance of *Toxoplasma gondii* infections in marine mammals: 2009-2020. *Veterinary Parasitology, 288*, 109296.
- Dubey, J.P. Toxoplasmosis: a waterborne zoonosis. (2004). *Veterinary Parasitology, 126*(1-2), 57-72.
- Dubey, J.P., Zarnke, R., Thomas, N., Wong, S.C., Bonn, W., Briggs, M.S., Davis, J.C., Ewing, R.C., Mense, M., Kwok, O.C, Romand, S., Thulliez, P. (2003). *Toxoplasma gondii, Neospora caninum, Sarcocystis neurona*, and *Sarcocystis canis*-like infections in marine mammals. *Veterinary Parasitology, 116*(4), 275-296.
- Frenkel, J.K. (1998). Pathophysiology of toxoplasmosis. *Parasitology Today, 4(*10), 273-278.
- Gonzales-Viera, O., Marigo, J., Ruoppolo, V., Rosas, F.C.W., Kanamura, C.T., Takakura, C.F.H, Fernández, A.Á., C Catão-Dias, J.L. (2013). Toxoplasmosis in a Guiana dolphin (*Sotalia guianensis*) from Paraná, Brazil. *Veterinary Parasitology, 191*(3-4), 358-362.
- Groch, K.R., Taniwaki, S.A., Favero, C.M., Brandao, P.E., Díaz-Delgado, J., Fernández, A., Catão-Dias, J.L., Sierra, E. (2020). A novel real-time PCR to detect Cetacean morbillivirus in Atlantic cetaceans. *Journal of Virological Methods, 285*, 113964.

- Herder, V., Van De Velde, N., Kristensen, J.H., Van Elk, C.E., Peters, M.D., Kilwinski, J., Schares, G., Siebert, U., Wohlsein, P. (2015). Fatal Disseminated *Toxoplasma gondii* Infection in a Captive Harbour Porpoise (*Phocoena phocoena*). *Journal of Comparative Pathology, 153*(4), 357-362.
- Ijsseldijk, L.L., Brownlow, A.C., Mazzariol, S. (2019). Best practice on cetacean post mortem investigation and tissue sampling.
- Inskeep, W.P., Gardiner, C., Harris, R.M., Dubey, J.P., Goldston, R.T., (1990). Toxoplasmosis in Atlantic Bottle-Nosed Dolphins (*Tursiops truncates*). *Journal of Wildlife Diseases, 26*(3), 377-382.
- Jones, T.C., Hunt, R.D., King, N.W. *Veterinary pathology. 6th ed. Ed. Baltimore, Md; London: Williams & Wilkins, 1997*. (s. f.).
- Kennedy, S. (1998). Morbillivirus infections in aquatic mammals. *Journal of Comparative Pathology, 119*(3), 201-225.
- Kochanowsky, J.A., Koshy, A.A. (2018). *Toxoplasma gondii*, *Current Biology, 28(*14): R770-R771.
- Kuiken, T., García Hartman, M. (1993). Cetacean pathology: dissection techniques and tissue sampling In: Newsletter, E. (Ed.), Proceedings of the First ECS Workshop on Cetacean Pathology, European Cetacean Society, Leiden, the Netherlands, p. Special Issue.
- Liu, Q., Wang, C., Huang, S., Zhu, X. (2015). Toxoplasmosis diagnosis and typing of *Toxoplasma gondii*. *Parasites and Vectors 8*(1).
- Massie, G.N., Ware, M., Villegas, E.N., Black, M.J. (2010). Uptake and transmission of *Toxoplasma gondii* oocysts by migratory, filter-feeding fish. *Veterinary Parasitology, 169*(3-4), 296-303.
- Migaki, G., Sawa, T.R., Dubey, J.P. (1990). Fatal disseminated toxoplasmosis in a spinner dolphin (*Stenella longirostris*). *Veterinary Pathology, 27*(6), 463-464.
- Milligan, S.A., Katz, M.S., Craven, P.C., Strandberg, D.A., Russell, I.J., Becker, R.C. (1984). Toxoplasmosis presenting as panhypopituitarism in a patient with the acquired immune deficiency syndrome. *The American Journal of Medicine, 77*(4), 760-764.
- Mikaelian, I., Boisclair, J., Dubey, J.P., Kennedy, D., Martineau, D. (2000). Toxoplasmosis in Beluga Whales (*Delphinapterus leucas*) from the St Lawrence

Estuary: Two Case Reportsand a Serological Survey. *Journal of Comparative Pathology, 122*(1), 73-76.

- Morell, M., IJsseldijk, L.L., Berends, A.J., Gröne, A., Siebert, U., Raverty, S., Shadwick, R.E., Kik, M. (2021). Evidence of Hearing Loss and Unrelated Toxoplasmosis in a Free-Ranging Harbour Porpoise (*Phocoena phocoena*). *Animals, 11*(11), 3058.
- Moro Abad, L., Martín Esquivel, J.L., Garrido Sanahuja, M.J., Izquierdo Zamora, I. (2003). List of marine species of the Canary Islands (algae, fungi, plants and animals). Consejería de Política Territorial y Medio Ambiente del Gobierno de Canarias (Regional Ministry of Territorial Policy and Environment of the Canary Islands Government).
- Prayson, N.F., Prayson, R.A. (2017). Toxoplasmosis of the pituitary gland. *Clinical Neuropathology.*
- Resendes, A.R., Almería, S., Dubey, J.P., Obón, E., Juan-Sallés, C., Degollada, E., Alegre, F., Cabezón, O., Pont, S., Domingo, M. (2002). Disseminated toxoplasmosis in a Mediterranean pregnant Risso's dolphin (*Grampus griseus*) with transplacental fetal infection. *J Parasitol 88*(5), 1029-1032.
- Roe, W.D., Howe, L., Baker, E.T., Burrows, L., Hunter, S.D. (2013). An atypical genotype of *Toxoplasma gondii* as a cause of mortality in Hector's dolphins (*Cephalorhynchus hectori*). *Veterinary Parasitology, 192*(1-2), 67-74.
- Sacristán, C., Carballo, M., Muñoz, M.J.R., Bellière, E.N., Neves, E., Nogal, V.D., Esperón, F. (2015). Diagnosis of Cetacean morbillivirus: A sensitive one step real time RT fast-PCR method based on SYBR(®) Green. *Journal of Virological Methods, 226*, 25-30.
- Sierra, E., Fernández, A., Felipe-Jiménez, I., Zucca, D., Díaz-Delgado, J., Puig-Lozano, R., Câmara, N., Consoli, F., Díaz-Santana, P.J., Suárez-Santana, C.M., Arbelo, M. (2020). Histopathological Differential Diagnosis of Meningoencephalitis in Cetaceans: Morbillivirus, Herpesvirus, *Toxoplasma gondii*, *Brucella sp*., and *Nasitrema sp*. *Frontiers in Veterinary Science, 7.*
- Van Bressem, M., Raga, J.A., Di Guardo, G., Jepson, P., Duignan, P.J., Siebert, U., Barrett, T., De Oliveira Santos, M.C., Moreno, I., Siciliano, S., Aguilar, A., Van

Waerebeek, K. (2009). Emerging infectious diseases in cetaceans worldwide and the possible role of environmental stressors. *Diseases of Aquatic Organisms, 86*, 143-157.

- Weidner, J.M., Barragán, A. (2014). Tightly regulated migratory subversion of immune cells promotes the dissemination of *Toxoplasma gondii. International Journal for Parasitology, 44*(2), 85-90.

- Zhang, X.Y., Li, Q.J., Hu, P., Cheng, H.C., Huang, G. (2002). Two case reports of pituitary adenoma associated with *Toxoplasma gondii* infection. *Journal of Clinical Pathology, 55*(12), 965-966.

ANNEX

Annex 1. Table 1. Collected samples and their method of preservation in alphabetical order.

COLLECTED SAMPLES		Animal number 1		Animal number 2	
		Method of preservation		Method of preservation	
TISSUES		Histology	Microbiology	Histology	Microbiology
Adrenal glands		X	X	X	X
Aorta		X		X	X
Blood					
Brain		X	X	X	X
CSF					
Diaphragm		X		X	X
Ear					
Esophagus		X		X	
Fluid	Blood		X		
	Cavity thoracic		X		
	Cavity abdominal		X		
	Pericardium		X		
	Urine		X		
Heart		X	X	X	X
Hypophysis		X		X	
Intestine		X	X	X	
Kidneys		X	X	X	X
Liver		X	X	X	X
Lungs		X	X	X	X
Lymphatic nodes	Mediastinal				
	Prescapular	X	X	X	X
	Pulmonary	X	X	X	X
	Tracheo-bronchial	X		X	X
	Mesenteric	X	X	X	X
	Rectal	X		X	
Pancreas		X		X	

Penis	X		X	
Prostate	X	X	X	
Rete mirabile	X	X	X	X
Skeletal muscle	X	X	X	X
Skin	X	X	X	X
Spleen	X	X	X	X
Spinal cord	X	X	X	X
Stomach 1	X		X	
Stomach 2	X		X	
Stomach 3	X		X	
Testicles	X	X	X	X
Thyroid	X		X	
Tongue	X		X	
Tonsils	X		X	
Trachea	X		X	
Urinary bladder	X		X	
Vitreous humor				
Others: Acoustic fat and muscle region fracture			X	
Others: Left pterygoid sac			X	X

Annex 2. Anatomopathological reports

- **Animal number 1:**

- External examination: Eight different types of lesions are observed in the skin:

Macroscopically:

A1: deep incised lesion affecting a blubbler (11.5 x 2 cm) on the right side, ventral to the beginning of the dorsal fin.

A2: multifocal dark circular lesions on dental interactions (rake marks) on the right side of the peduncle, dorsal to the genital area.

A3: whitish multifocal lesions arranged close to each other (3 x 2 mm) dorsal to the genital area on the peduncle on the right side.

A4: focal lesion similar to A3 located caudal to the anal area on the right side.

A5.1 and A5.2: Interspecific interaction marks arranged parallel to each other on the dorsal fin and left side (1 - 1.5 cm interdental space, possibly interaction with bottlenose dolphin).

A6: focal lesion similar to A3 and A4 but without being located on "rake marks" on the left side of the peduncle with a diameter of 1.5 cm.

A7: dark lesion that is apparently the result of several lesions that have merged together, with an isolated lesion close to the dorsal part of the caudal peduncle with a length of 7 cm.

A8: lesion similar to A5 located ventral to it.

Microscopically: A1: diffusely, intercellular edema is observed in the spinous layer, increasing the space between the keratinocytes, observing the intercellular bridges. In addition, a lighter color change can be seen throughout the entire layer. Multifocally, a loss of continuity of the skin is observed, observing moderate hemorrhage and a slight granulomatous inflammatory infiltrate with fibrin in the nearby areas.

A2: diffusely, hyperplasia of the spinous layer is observed, with a thickening of the epidermal ridges, giving rise to their lateral union. Moderate increase in the number of melanocytes in the most basal zone of the epidermal ridges, acquiring a rounded appearance. Moderate presence of koilocytes.

A3: focalized hyperplasia. Digitization of the epidermal ridges towards the dermis.

A4: diffuse hyperplasia with digitalization of the epidermal ridges towards the dermis.

A5: multifocal neutrophilic inflammatory infiltrate with diffuse hemorrhage affecting both the stratum spinosum of the epidermis and the dermis. Loss of the stratum corneum in a

multifocal manner. High melanin content in the stratum spinosum, affecting the basal area of the epidermal ridges to a greater extent.
A6: mild diffuse hyperplasia with digitalization of the epidermal ridges towards the dermis.
A7: diffuse hyperplasia with slight multifocal vacuolization of the keratinocytes within the epidermal ridges.
A8: Mild diffuse hyperplasia, with multifocal neutrophilic infiltrate in the epidermal ridges, which were observed to be edematous.

- Subcutaneous tissue: Macroscopically, there is an emphysematous appearance with congestion and diffuse yellowish appearance of the fat. It has a crepitant consistency, while cutting through the layers of skin and fat reveals a large amount of blood that does not coagulate.

- Musculoskeletal system: Macroscopically, it presents a dark reddish color that, when cut, shows a lot of blood. Multifocally, there is a slight presence of parasitic cysts compatible with *Monorygma* sp. And microscopically, on the longest part of the back, it can be seen a mildly multifocal, lymphohistiocytic infiltrate with macrophages and interstitial edema is observed. Presence of mild acute degenerative changes (segmental necrosis). Focally, a large cyst compatible with *Sarcocystis* sp. In the rectus abdominis, it can be seen a large, elongated cyst compatible with *Sarcocystis* sp. is observed in a multifocal manner. Moderate acute myodegenerative changes (segmental and discoid degeneration, hypercontraction, hyperacidophilia, accordion fibers) and presence of myocyte nuclei in a multifocal row. And in the diaphragm, it can be seen a mild to moderate acute multifocal myodegenerative changes (segmental and discoid degeneration, hypercontraction, hyperacidophilia, accordion fibers).

- Thoracic cavity: Macroscopically, a low content of orange-coloured serous fluid is present.

- Respiratory system: Macroscopically, in the larynx, it can be seen a diffuse reddish color changes. In the windpipe, a small amount of blood is observed. And in the lung, the left lung appears slightly reduced in size with a more reddish coloration, while the right lung appears enlarged. Color changes with multifocal whitish areas are observed in both.While, microscopically, it can be seen a moderate multifocal presence of intracellular protozoan cysts (*Toxoplasma* sp) in smooth muscle fibers of bronchi and bronchioles. In a diffuse and severe

way, a lymphoplasmacytic infiltrate is observed bronchointerstitial. In alveolar lumens, presence of moderate edema, foamy macrophages and occasional presence of multinucleated cells (acute lymphoplasmacytic interstitial bronchopneumonia). Presence of moderate diffuse edema at the interstitial, subpleural and perivascular level. Multifocal thickening of the pleura. Areas of moderate multifocal interstitial fibrosis with associated angiomatosis. Moderate multifocal intra-alveolar hemorrhages. Moderate enlargement of the alveolar spaces in a multifocal manner (pulmonary emphysema) with the occasional presence of nematodes inside them. Bacillary bacteria are mildly observed in the lung parenchyma. Multifocal areas of necrosis and mineralizations in the submucosa of bronchi and bronchial tubes in a mild multifocal manner are seen.

- Cardiovascular system:

- Heart: Macroscopically, in the left atrium there is the presence of a clot adhered to the atrioventricular valves. And microscopically, it can be seen a moderate multifocal presence of protozoan cysts compatible with *Toxoplasma* sp. in the sarcoplasm of cardiomyocytes with mild associated lymphoplasmacytic infiltrate. Edema and moderate multifocal interstitial hemorrhages, with the presence of fibrosis and mild multifocal granulomatous infiltrate are seen. Occasionally intracytoplasmic vacuolizations are observed. Moderate multifocal acute myodegenerative changes (segmental necrosis) and chronic changes (moderate multifocal cardiomyocyte atrophy) are seen. In a slight random manner, mineralizations of different sizes are seen in the muscle fibers.
- Large glasses: Macroscopically, the wall of the aorta appears congested. And microscopically, in the aorta it can be seen a moderate interstitial hemorrhage with mild neutrophilic-granulomatous infiltrate. Presence of diffuse intravascular and extravascular edema with perivascular fibrin and moderate vessel wall thickening with vascular dilation and moderate intravascular congestion are seen. While, in the rete mirabile, it can be seen a diffuse moderate interstitial hemorrhage with granulomatous infiltrate and intracytoplasmic tachyzoites compatible with *Toxoplasma* sp.

- Digestive system:

- Oral cavity: Macroscopicaly, in the ventral part of the tongue, a dark-green, oval, raised focal lesion (10x15 mm) of soft consistency can be seen that, when cut, summarizes pasty dark-green content. In the apical part, multifocal, ulcerative, circular lesions (4 x 4 mm)

with clear, depressed centers with loss of epithelium and a dark-greenish halo are observed. And microscopically, in a focally extensive manner, loss of the lingual epithelium is observed with severe epithelial necrosis affecting the mucosa and submucosa, cellular debris, fibrin, and underlying brownish granulation tissue (necrotic-ulcerative glossitis) with bacteria and moderate associated vascular changes. Vacuolization of the cytoplasm of the marginal epithelial cells with vesicle formation in a multifocal manner. Muscular atrophy with lymphohistiocytic infiltrate, degenerated neutrophils, and bacillary bacteria is seen. Presence of inflammatory infiltrate with a predominance of polymorphonuclear cells affecting the vascular wall (vasculitis). Fibrin and hyaline degeneration are observed in the vessel wall. In the musculature there is presence of moderate multifocal hemorrhages. The nuclei of the myocytes are enlarged and apparently protruding one side of the cell wall in a marked multifocal manner.

- Pharynx: Macroscopically, it can be seen a thickened, congestive mucosa with presence of whitish mucus.

- Esophagus: Macroscopically, the presence of cloudy whitish content of dense consistency is observed.

- Stomach: Macroscopically, it can be seen multifocal areas of bright red coloration with an edematous appearance are observed in the mucosa. Mucous content is appreciated. And microscopically, in a multifocal manner, loss of continuity of the mucosa and muscle layer is observed with moderate lymphoplasmacytic infiltration associated with the presence of various nematode parasites (*Anisakis* sp). In multifocal surrounding areas, mild multifocal necrosis and fibrin (ulcerative gastritis) is observed.

- Pyloric stomach: Macroscopically, an oval area with a hard consistency is observed, with depressed edges, yellowish coloration, affecting transmurally, being highly compatible with a parasitic cyst (*Pholleter* sp). And microscopically, a multifocally, loss of mucosal continuity (ulcer) is observed, with fibrin deposits and associated mineralizations and moderate multifocal areas of necrosis. In the submucosa there is moderate granulomatous infiltration, associated with the presence of several trematode parasites (*Pholleter* sp) surrounded by connective tissue. In this same layer, the presence of intravascular thrombi can be observed, causing complete occlusion of the lumen (phlebitis) with surrounding marked neovascularization. In multifocal surrounding areas, mild multifocal necrosis and fibrin (ulcerative gastritis) is observed. At the level of the muscle layer, in the interstitium, a mainly mononuclear diffuse infiltrate with

macrophages with multifocal brownish pigment (remnants of parasites) is observed. Acute myodegenerative changes (hypercontraction and hyperacidophilia) and mild multifocal fibrosis are observed in muscle fibers. There is thickening of the serosa with increased connective tissue, edema, and a diffuse mononuclear infiltrate.

- Duodenal ampulla: Macroscopically, contracted areas compatible with rigor mortis are observed in a multifocal manner. The serous vessels appear congested. In a disseminated way, the presence of large and small caliber air bubbles in the mesenteric vessels is observed. And microscopically, it can be seen the presence of a moderate multifocal lymphoplasmacytic infiltrate in the mucosa associated with hemorrhage. Likewise, in the mucosa, the formation of horny pearls is observed in a moderate multifocal manner. Presence of short apical bacillary bacteria in a moderately diffuse manner in the intestinal mucosa. The muscularis vessels present intravascular thrombi in a moderate multifocal manner.

- Proximal intestine: The same macroscopic and microscopic lesions are observed as in the duodenum.

- Middle intestine: The same macroscopic and microscopic lesions are observed as in the duodenum.

- Distal intestine: Macroscopically, the same lesions are observed as in the rest of the intestine, while microscopically it can be seen the presence of a moderate multifocal lymphoplasmacytic infiltrate in the mucosa associated with hemorrhage. Likewise, in the mucosa, the formation of horny pearls is observed in a moderate multifocal manner. Presence of short apical bacillary bacteria in a moderately diffuse manner in the intestinal mucosa. The muscularis vessels present intravascular thrombi in a moderate multifocal manner. In the anal tonsil, in the lumen of a crypt focus, parasitic structures compatible with the larval stage of cestodes can be observed.

- Pancreas: Macroscopically, it is observed increased in size with rounded edges. There is a multifocal presence of light-colored areas surrounded by a reddish halo with irregular edges that deepens into the parenchyma. The pancreatic duct is seen dilated with dark-red content of a dense consistency. Associated parasites (trematodes) can be seen. The vessel associated with the pancreas is dilated with a high gas content. And microscopically, it can be seen a severe multifocal-coalescing necrosis of the parenchyma with associated multifocal hemorrhages. Mild presence of intracytoplasmic protozoan cysts compatible with *Toxoplasma*

sp and multifocal presence of intracanicular flukes associated with moderate hemorrhage and moderate-severe pyogranulomatous infiltrate are seen. Diffusely, there is marked hyperplasia of the epithelium of the pancreatic ducts, fibrosis, and lymphoplasmacytic infiltrate (ductitis). The capsule is diffusely expanded with a perivascular lymphoplasmacytic infiltrate. Interstitial connective tissue proliferation (fibrosis) is seen. Glandular dilatation with accumulation of mucus in a multifocal manner.

- Liver: Macroscopically, it can be seen an increased in size with rounded edges of dark colouring. When cut summarize high blood content. The vessels of the hepatic vein are dilated with a high presence of gas and without clotted blood. And microscopically, a moderate sinusoidal multifocal hemorrhage with midzonal congestion is observed. Multifocal areas where hepatic architecture is lost associated with an inflammatory infiltrate with degenerated cells, with randomly dispersed multifocal hepatic necrosis are observed. Moderate multifocal presence of protozoan cysts compatible with *Toxoplasma* sp. in the cytoplasm of hepatocytes. Diffuse biliary hyperplasia is observed in a moderate way. Concentric fibrosis around the hepatic ducts with enlarged spaces and lymphoplasmacytic infiltrate (cholangitis). In a severe diffuse manner, vacuolization of the hepatocytes is observed, presenting intracytoplasmic pigment deposit (hemosiderin).

- Urinary system:

  - Kidneys: Macroscopically, it can be seen a diffuse bilateral perirenal emphysema. And microscopically, it can be see congestion and interrenicular hemorrhages. At the level of the cortex, dense accumulations of multifocal lymphoplasmacytic infiltrate that expands into the interstitium (interstitial nephritis). Multifocally, areas of mild necrosis can be seen. Multifocal hyaline casts are observed at the medullary level. Moderately, there is a multifocal thickening of Bowman's membrane with occasional sclerotic glomeruli and mineralization of the glomerulus.
  - Urinary bladder: Macroscopically, it can be seen a diffuse congestion and thickening of the wall. And microscopically, it can be seen a marked congestion and diffuse moderate edema affecting the serosa.

- Reproductive system

  - Epididymis: Macroscopically, presense of *Monorygama grimaldii cyst* are seen.

- Penis: Microscopically, there is moderate diffuse acanthosis with hyperplasia of the irregular basal outer layer.

- Prostate: Microscopically, mild moderate multifocal fibrosis with mild prostatic hyperplasia is observed.

- Lymphoid system

- Spleen: Macroscopically, it is observed increased in size with the multifocal presence of raised dark nodules, mostly located in the cortex. And microscopically, marked lymphoid depletion of the white splenic pulp, moderate-severe multifocal lymphocytolysis is observed.

-Pharyngeal tonsil: Microscopically, moderate lymphoid hyperplasia with hyalinization of the lymphoid follicles is observed. In addition, markedly, diffuse vascular congestion is observed. At the level of the crypts, short bacillary bacteria can be seen with occasional macrophages and neutrophils in the pharyngeal crypts.

- Laryngeal tonsil: Macroscopically, it can be seen a diffuse congestion is observed as well as bright-red coloration. And microscopically, a marked congestion and edema. And multifocal presence of dilated crypts with acidophilic colloidal material are seen. Moderate lymphoid hyperplasia with hyalinization of the lymphoid follicles is observed. Focal presence of parasitic structure compatible with nematode. Presence of infiltrate with occasional neutrophils and binucleated cells, amorphous anuclear material, abundant macrophages and bacteria in the lumen of the tonsillar crypts. Fibrosis and mild multifocal angiomatosis.

- Preescapular lymph node: Macroscopically, they are enlarged. The presence of edema in surrounding tissue is observed as well as hemorrhage. When cut, the presence of irregular areas with a reddish border with a clear interior and a gray-greenish delimitation is observed in a multifocal manner. And microscopically, a multifocal venous dilation associated with a dilation of the surrounding lymphatic vessels can be seen. In a multifocal manner, the presence of fibrin deposits in peritrabecular spaces and sinusoidal hemorrhage is observed. Moderate-severe sinus histiocytosis is seen. At the capsular level, moderate lymphoplasmacytic infiltrate with moderate hemorrhage, also affecting the subcapsular level. Hemorrhages and moderate diffuse blood resorption are noted.

- Tracheobronchial lymph node: Microscopically, moderate and diffuse multifocal lymphoid depletion is observed. In a multifocal manner, the presence of fibrin deposits

and sinusoidal hemorrhage is observed. At the capsular level, a moderate lymphoplasmacytic infiltrate with moderate hemorrhage can be seen, also affecting the subcapsular level. Presence of inflammatory infiltrate with a predominance of polymorphonuclear cells affecting the vascular wall with the presence of endothelial edema (vasculitis).

- Pulmonary lymph node: Macroscopically, bilaterally, they are enlarged with a generalized dark coloration and edematous. And microscopically, it can be seen a mild depletion. In a moderate diffuse manner, the presence of foamy macrophages with an accumulation of brownish pigment can be seen throughout the lymphoid tissue and with the occasional presence of multinucleated cells. Diffuse marked congestion and moderate sinus histiocytosis is noted. Moderate multifocal travecular perivascular space expansions.

- Mesenteric lymph node: Macroscopically, they are observed enlarged with a dark gray coloration. And microscopically, the presence of multifocal cavitations in the renal medulla is clearly observed. Moderate multifocal lymphoid depletion and congestion is seen with macrophages containing brownish pigment and moderate multifocal medullary fibrin. Mild multifocal sinus histiocytosis, the cytoplasm of macrophages presents abundant brownish pigment.

- Rectal lymph node: Microscopically, a multifocal moderate sinus histiocytosis is seen. Enlarged subcapsular and travecular spaces with abundant multifocal presence of macrophages.

- Other lymph nodes: Macroscopically, the aortic lymph node is shown enlarged. And microscopically, the presence of perivascular hemorrhage is observed in a moderate multifocal manner, in addition to appreciating the diffuse thickening of the perivascular tunica in an accentuated manner. The presence of macrophages with accumulation of brownish pigment (hemosideromacrophages) with multifocal short bacillary bacteria is observed diffusely throughout the lymphoid tissue. Moderate multifocal blood resorption and multifocal presence of areas of necrosis can be seen. Mild presence of multifocal sinus histiocytosis.

- Endocrine system:

  - Adrenal glands: Macroscopically, bilaterally, the cortex is thickened, with multifocal changes affecting both the cortex and the medulla. Likewise, in both adrenal glands the presence of a focal dilation (2 mm) in the medulla is observed. And microscopically, bilaterally, severe multifocal presence of areas of necrosis, hemorrhages and lymphocytic infiltrate affecting cortex and medulla, associated with intracytoplasmic protozoan cysts and extracellular zoites compatible with *Toxoplasma* sp (necrotizing adrenalitis). Congestion and marked edema. Mild multifocal fibromyxomatous degeneration.

  - Hypophysis: Microscopically, it can be seen intracytoplasmic protozoan cysts and extracellular zoites compatible with *Toxoplasma* sp. And diffuse marked congestion.

- Sense organs:

  - Pterygoid sacs: Macroscopically, bilateral presence of trematode parasites. The mucosa appears diffusely red with associated brownish discharge. And microscopically, it can be seen a multifocal presence of trematode parasites and triangular eggs compatible with *Nasitrema* sp. in the lumen of the pterygoid sacs. The eggs are also embedded in the submucosa. Presence of severe multifocal hemorrhages. Severe moderate multifocal intravascular coagulation.

- Central nervous system:

  - Spinal cord: Microscopically, it can be seen a multifocal presence of non-suppurative areas of inflammatory infiltrate in the meninges and neuropil with loss of tissue structure in all areas of the brain associated with the presence of intracytoplasmic protozoan cysts and extracellular zoites compatible with Toxoplasma *sp* . Diffusely, a marked proliferation of astrocytes (gliosis) is observed. Loss of normal cortical structure due to marked diffuse spongiosis, giving rise to multifocal vesicles. Presence of multifocal hemorrhages and perivascular edema with associated globular astrocytes.

  - Brain: Macroscopically, it can be seen a moderate congestion with presence of air bubbles in a severe way. And microscopically, it can be seen a multifocal presence of non-suppurative inflammatory infiltrate areas in the meninges and neuropil with loss of tissue structure in all areas of the brain associated with the presence of intracytoplasmic protozoan cysts and extracellular zoites compatible with *Toxoplasma*

sp. Diffusely, a marked proliferation of astrocytes (gliosis) is observed. Loss of normal cortical structure due to marked diffuse spongiosis, giving rise to multifocal vesicles. Presence of multifocal hemorrhages and perivascular edema with associated globular astrocytes.

- Cerebellum: Microscopically, it can be seen a multifocal presence of non-suppurative inflammatory infiltrate areas in the meninges and neuropil with loss of tissue structure in all areas of the brain associated with the presence of intracytoplasmic protozoan cysts and extracellular zoites compatible with Toxoplasma *sp.*

- **Animal number 2:**

- External exam: Macroscopically, it can be seen multiple linear, parallel, surface markings, compatible with intra/interspecific interaction markings on the body surface. On the face, multiple erosions/ulcers with associated color changes in the surrounding tissues. On the left side, area of deformation, with a dark red color change. In addition, a circular skin lesion (A1) with a dark center and light halo, smooth surface, 15x15mm, is observed on the lateral side of the right caudal peduncle. Moderate presence of *Phylobothrium delphini cysts* in blubber of the genital region and caudal peduncle. And microscopically, in the deep hypodermis, moderate multifocal presence of hemorrhages, moderate edema and mononuclear infiltrate (lymphocytes and macrophages) (granulomatous panniculitis) are seen.

A1: Focal area of fibrosis. In the deep hypodermis, interstitial edema and slight presence of mononuclear infiltrate, mild congestion and mild multifocal intravascular coagulation.

- Subcutaneous tissue: Macroscopically, it can be seen a marked edema and emphysema in the cervical and left scapular region and a marked serous atrophy of fat in the cervical region.

- Musculoskeletal system: Macroscopically, in the scapular region of the left side, moderate edema and hemorrhages in muscle masses are seen. Marked diffuse hemorrhages in the muscles and soft tissues of the mandibular region, associated with a bilateral fracture of the body of the mandible. Comminuted fractures at the level of the tympanic-periotic complex on the left side. Mild presence of *Crassicauda* sp. very long on the back and slight presence of *Monorygma grimaldii cysts* in the rectus abdominis. Microscopically, in the rectus abdominis, it can be seen a mild presence of acute degenerative changes (hypercpntraction and

hyperacidophilia). And in the jaw fracture region muscle, it can be seen moderate multifocal haemorrhages.

- Respiratory system:

- Trachea: Macroscopically, it can be seen a moderate presence of bloody and foamy fluid in the trachea and bronchi and multifocal hemorrhages are seen in the submucosa of the major bronchi.

- Lungs: Macroscopically, both lungs appear congested, with multifocal areas of mild atelectasis. When cut, the parenchyma oozes a moderate amount of foamy fluid (alveolar edema). And microscopically, it can be seen a marked congestion, moderate generalized atelectasis, mild to moderate multifocal alveolar hemorrhages, mild alveolar edema with associated foamy macrophages, mild multifocal interstitial lymphoplasmacytic infiltrate with occasional presence of multinucleated cells in alveolar lumens (interstitial pneumonia). A section shows a focus of necrosis, vasculitis, associated lymphoplasmacytic infiltrate, and abundant foamy macrophages. Another section shows a focus of lymphoplasmacytic infiltrate and the presence of amorphous, acidophilic material with necrotic cells in the center. At the level of the submucosa of large caliber bronchi, marked congestion and edema. Moderate multifocal mineralizations in the submucosa of bronchi and bronchioles are seen.

- Cardiovascular system:

- Heart: Microscopically, it can be seen a moderate multifocal presence of lymphoplasmacytic infiltrate in myocardium, mainly at the level of the atria associated with necrosis of cardiomyocytes with occasional presence of protozoan cysts (bradyzoites) compatible with *Toxoplasma gondii*. Congestion and marked interstitial edema. Moderate multifocal presence of lymphoplasmacytic infiltrate in epicardium and in interstitial tissue, surrounding blood vessels. Moderate congestion and mild multifocal leukocytosis are seen.
- Large vessels: Microscopically, in the thoracic aorta, in the adventitia, moderate multifocal presence of lymphoplasmacytic infiltrate and edema separating connective tissue fibers are seen.
- Rete mirabile: Microscopically, it can be seen a moderate multifocal presence of lymphoplasmacytic infiltrate in interstitial, perivascular and perineural tissue,

associated with the moderate presence of protozoan cysts (bradyzoites), compatible with *Toxoplasma gondii* within the cytoplasm of fibroblasts. Moderate multifocal vasculitis. A marked congestion is seen.

- Abdominal cavity: Macroscopically, it can be seen a moderate presence of *Monorygma grimaldii cysts* , mostly in the genital region.

- Digestive system:

- Oral cavity: Macroscopically, it can be seen a multiple broken teeth and a moderate multifocal presence of ulcers on the dorsal surface of the tongue. Congestive oral mucosa is seen. And microscopically, in the tongue, it can be seen a moderate multifocal presence of ulcers, with areas of necrosis of the mucosa and areas where the cells present intracellular and intercellular edema, areas of necrosis at the level of the submucosa, severe hemorrhages both at the superficial level and at the level of the submucosa, moderate infiltrate of polymorphonuclear cells in the submucosa and abundant intralesional bacteria. Abundant desquamated cells are observed in the lumen of the lingual glands, some binucleate macrophages.

- Esophagus: Microscopically, it can be seen a slight presence of protozoan cysts (bradyzoites), compatible with *Toxoplasma gondii* in striated muscle fibers, slight presence of lymphoplasmacytic infiltrate, multifocal in the submucosa, focal vasculitis.

- Keratinized stomach: Macroscopically, it can be seen a scarce squid beaks and otoliths and a multifocal presence of ulcers of 1-2 mm. Microscopically, it can be seen a focal ulcer in the mucosa with traces of digested blood, epithelial necrosis and little inflammatory reaction. Moderate multifocal presence of areas of lymphoplasmacytic infiltrate in muscle layers, necrosis and multifocal vasculitis, associated with the presence of protozoan cysts (bradyzoites), compatible with *Toxoplasma gondii* in smooth muscle fibers.

- Main stomach: Microscopically, it can be seen a mild multifocal presence of lymphoplasmacytic infiltrate in the mucosa, submucosa, and muscle. In the muscle layer, slight presence of protozoan cysts (bradyzoites), compatible with *Toxoplasma gondii* in the cytoplasm of myocytes.

- Pyloric stomach: Microscopically, it can be seen a moderate multifocal presence of lymphoplasmacytic infiltrate associated with foci of necrosis in the submucosa and muscle layer, with a moderate presence of protozoan cysts (bradyzoites), compatible with *Toxoplasma gondii* in the cytoplasm of muscle fibers and in fibroblasts of interstitial tissue. Focal presence of parasitic eggs in the submucosa surrounding a nerve.

- Duodenal ampulla: Macroscopically, it can be seen a mild multifocal presence of petechiae on the mucosa. Mild presence of nematode parasites. And microscopically, it can be seen a mild multifocal presence of lymphoplasmacytic infiltrate associated with foci of necrosis in the muscle layer.

- Proximal intestine: Microscopically, it can be seen a mild multifocal presence of lymphoplasmacytic infiltrate in the muscle layer and Auerbach's plexus, with slight presence of protozoan cysts (bradyzoites), compatible with *Toxoplasma gondii* within muscle fibers and neuronal somata. In the light, a parasitic structure is observed.

- Middle intestine: Microscopically, we can see the same lesions present in the proximal intestine.

- Pancreas: Macroscopically, it can be seen a moderate number of flukes in the lumen of pancreatic ducts. And microscopically, it can be seen a moderate multifocal presence of flukes in the lumen of pancreatic ducts and fibrosis of the ductal wall.

- Liver: Macroscopically, it can be seen a slight amount of flukes (N:2) in the main hepatic duct. And microscopically, it can be seen a marked congestion and a mild multifocal lymphoplasmacytic periportal hepatitis. In the cytoplasm of the hepatocytes, moderate presence of vacuolizations and brownish pigment.

- Urinary system:

- Kidneys: Microscopically, in the capsule, moderate perineural and perivascular lymphoplasmacytic infiltrate are seen. Diffuse marked congestion. In cortex, multifocal presence of interstitial lymphohistiocytic infiltrate, sometimes forming pseudofollicles, associated with parasitic structures (nematode larvae). In the medulla, multifocal presence of mineralizations of the tubules.

- Bladder: Microscopically, it can be seen a mild multifocal presence of perivascular lymphoplasmacytic infiltrate and associated foci of necrosis in the muscle layer, with a moderate presence of protozoan cysts (bradyzoites), compatible with *Toxoplasma gondii* within muscle fibers.

- Reproductive system:

- Penis: Microscopically, it can be seen a mild multifocal lymphoplasmacytic infiltrate in the submucosa.

- Prostate: Macroscopically, it can be seen a mild to moderate presence of nematode parasites. And microscopically, it can be seen a moderate nematodes in the lumen of prostate glands, prostatic duct and in skeletal muscle. Focal presence of pyogranuloma in muscle. At the level of the skeletal muscle, lymphoplasmacytic infiltrate and moderate presence of protozoan cysts (bradyzoites), compatible with *Toxoplasma gondii* within muscle fibers.

- Endocrine system:

- Hypophysis: Macroscopically, it can be seen a marked hemorrhages at the level of plexuses and surrounding tissues. And microscopically, it can be seen an area of severe necrosis, focally extensive, at the level of the adenohypophysis, abundant lymphoplasmacytic infiltrate with abundant macrophages in the parenchyma, the capsule and in the interstitium of the associated vascular plexus.

- Thyroid: Macroscopically, it can be seen a congestion and generalized edema. And microscopically, in the capsule, moderate multifocal presence of lymphoplasmacytic infiltrate associated with protozoan cysts (bradyzoites) compatible with *Toxoplasma gondii* in the cytoplasm of endothelial cells and fibroblasts are seen. Moderate multifocal hemorrhages at the level of peripheral tissues and a marked congestion are seen.

- Adrenal glands: Macroscopically, bilateral corticomedullary junction hemorrhages and bilateral cortical hyperplasia are seen. And microscopically, it can be seen a moderate to severe multifocal presence of areas of necrosis with lymphoplasmacytic infiltrate, associated with the presence of protozoan cysts (bradyzoites) compatible with *Toxoplasma gondii* in the capsule, septa, cortex, and adrenal medulla. Bradyzoites are seen in fibroblasts, cells of the

adrenal cortex and medulla, and nerve capsule. Mild multifocal lymphoplasmacytic neuritis. Mild multifocal vasculitis and a marked congestion are seen.

- Lymphoid system:

  - Spleen: Microscopically, it can be seen a moderate multifocal centrofollicular hyalinosis and depletion. Moderate presence of macrophages with orange/brown intracytoplasmic pigment.

  - Preescapular lymph node: Macroscopically, it can be seen edematous and congestion. And microscopically, it can be seen a marked congestion. Moderate lymphoid depletion marked sinus histiocytosis. Blood resorption and erythrophagocytosis. Abundant dilations with negative staining in the sinuses and parenchyma.

  - Tracheobronchial lymph node: Microscopically, it can be seen an absence of lymphoid follicles, severe multifocal hyalinosis, severe sinus histiocytosis. At the level of the capsule, multifocal presence of lymphoplasmacytic infiltrate.

  - Pulmonary lymph node: Microscopically, it can be seen a marked congestion. Severe lymphoid depletion with absence of cortical follicles and moderate multifocal areas of hyalinization and necrosis. Marked sinus histiocytosis. Presence of nematodes in the capsule and in the parenchyma with associated multinucleated cells. Negatively staining dilations in subcaspular sinuses.

  - Mesenteric lymph node: Microscopically, it can be seen a marked lymphoid depletion and moderate multifocal centrofollicular hyalinization.

  - Rectal lymph node: Microscopically, it can be seen a marked lymphoid depletion and moderate multifocal centrofollicular hyalinization.

  - Pharyngeal tonsil: Microscopically, it can be seen a marked lymphoid depletion with severe multifocal hyalinosis. Loss of epithelial structure with abundant desquamated cells and multifocal hemorrhages in the mucosa and submucosa. Mild multifocal lymphoplasmacytic myositis with the presence of intracytoplasmic granular basophilic material in myocytes. In a crypt, an accumulation of compact, acellular brownish/yellowish material is observed.

  - Laryngeal tonsil: Microscopically, in the crypts, severe multifocal presence of neutrophilic and macrophage exudate with occasional multinucleated cells, hemorrhages, and abundant round-oval, basophilic, 2-3 micron structures are seen.

Mild multifocal presence of parasitic larvae in a crypt. Moderate multifocal presence of areas of necrosis with intralesional bacteria. Slight multifocal mineralizations. Lymphoid depletion and marked multifocal hyalinosis.

- Anal tonsil: Microscopically, it can be seen dilated crypts, hyperplastic and desquamated epithelium and abundant larval stages of tetraphylloid cestodes (plerocercoids), some of them located below the basal membrane.

- Sense organs: Presence of conjunctival/ocular haemorrahges.

- Acoustic system: Macroscopically, it can be seen a comminuted fractures in the left tympanic-periotic complex, with surrounding soft tissue hemorrhages. Extensive hemorrhages at the level of the left mandibular acoustic fat, consistent with a fracture of the mandible. Microscopically, it can be seen a moderate multifocal hemorrhages in left mandibular acoustic fat.

- Pterygoid sacs: Macroscopically, it can be seen a diffuse hemorrhages on the left side. And microscopically, in the left pterygoid sac, marked congestion, moderate multifocal intravascular coagulation, moderate multifocal hemorrhages in the submucosa and mild in the muscle are seen.

- Central nervous system:

- Brain: Macroscopically, it can be seen a general congestion. The brain tissue presents generalized pale coloration. And microscopically, it can be seen a severe multifocal presence of areas of loss of tissue structure (necrosis) with non-suppurative inflammatory infiltrate, presence of lymphoplasmacytic perivascular cuffs, vasculitis, gliosis, neuronophagia and astrocytes with intracytoplasmic yellowish pigment, associated with the presence of numerous protozoan cysts and compatible free tachyzoites with *Toxoplasma gondii*. Foci of gliosis and isolated lymphoplasmacytic perivascular cuffs not associated with the presence of cysts are observed. Moderate multifocal vasculitis.

- Cerebellum: Macroscopically, it can be seen a marked congestion. And microscopically, it can be seen a moderate protozoan cyst compatible with *Toxoplasma gondii* in the Purkinje cell layer. Discrete foci of gliosis and mild lymphoplasmacytic meningitis are observed. Congestion and marked perivascular edema.

- Brainstem: Microscopically, it can be seen a severe multifocal presence of areas of loss of tissue structure (necrosis) with non-suppurative inflammatory infiltrate, presence of lymphoplasmacytic perivascular cuffs, vasculitis, gliosis, neuronophagia and astrocytes with intracytoplasmic yellowish pigment, associated with the presence of numerous protozoan cysts and compatible free tachyzoites with *Toxoplasma gondii*. Foci of gliosis and isolated lymphoplasmacytic perivascular cuffs not associated with the presence of cysts are observed. Moderate multifocal vasculitis.